91602
new 82-10

LEGAL NOTICE

This report was prepared by Ontario Hydro and, while effort has been made to assure the accuracy and applicability of the material contained herein, neither Ontario Hydro nor any person acting on its behalf:

(a) makes any warranty, express or implied with respect to the use of any information, apparatus, method or process disclosed in this report or that such use may not infringe privately owned rights; or

(b) assumes any liabilities with respect to the use of, or for damages resulting from the use of, any information, apparatus, method or process disclosed in this report.

ontario hydro
research division

# A DEMONSTRATIVE IMPACT ANALYSIS OF THE CONCRETE INTEGRATED CONTAINER

Report No. 89-286-K

H.P. (Jack) Lee
Engineer
Applied Mechanics Section
Mechanical Research Department

## ABSTRACT

An impact analysis of an irradiated fuel container to simulate an accidental drop onto an unyielding surface has been illustrated. The container which is composed of a thick concrete tank, enclosed both outside and inside by steel liners, is modelled and analyzed using the finite element technique. The interactive engineering software PATRAN is used for pre- and post-processing while the analysis is carried out using the hydrodynamic code DYNA3D. Results in terms of energy, momentum, contact force, stresses, strains and deformation during and after impact are demonstrated. It is concluded that the damage to both liners and concrete are localized in the vicinity of contact. Stresses decrease rapidly toward remote areas and become insignificant. An impact limiter composed of effective energy absorption material will eliminate damage to the container itself.

JC
AC

| job | file | date | report no. |
|---|---|---|---|
| 21-234-461 | 825.122 | January 8, 1990 | 89-286-K |

# TABLE OF CONTENTS


| | | Page |
|---|---|---|
| 1.0 | INTRODUCTION | 1 |
| 2.0 | GEOMETRY OF THE CONTAINER | 1 |
| 3.0 | MATERIAL PROPERTIES OF THE CONTAINER | 2 |
| | 3.1 Concrete | 2 |
| | 3.1.1 Stress-Strain Relation | 2 |
| | 3.1.2 Equation of State | 3 |
| | 3.2 Steel Liner | 3 |
| 4.0 | FINITE ELEMENT MODELING OF THE CONTAINER | 4 |
| 5.0 | ANALYTICAL RESULTS AND DISCUSSIONS | 4 |
| 6.0 | CONCLUSIONS | 6 |
| 7.0 | FUTURE WORK | 7 |
| REFERENCES | | 7 |
| FIGURES | | |
| APPENDIX A | | |
| DISTRIBUTION | | last page |

ontario hydro
research division

To Mr. P.D. Stevens-Guille
Radioactive Materials Management
Nuclear Engineering Department
Design and Development Division

# A DEMONSTRATIVE IMPACT ANALYSIS OF THE CONCRETE INTEGRATED CONTAINER

## 1.0 INTRODUCTION

The Nuclear Engineering Department is currently investigating the use of a reinforced concrete integrated container (CIC) for the dry storage, transportation and possible final disposal of irradiated fuel. One major consideration in this investigation is the assurance of its structural integrity in the event of an accidental drop of the container during transportation. Such an investigation can be carried out thoroughly using an analytical approach where the historical response of the container during its impact onto the ground can be recorded and studied. This report demonstrates a bench mark analysis of such a drop and illustrates its response during and after impact. The objective of this exercise is to achieve the following:

1. To provide detailed information to support the design of the container.

2. To explore the capability of using an analytical approach to investigate the container.

3. To serve as a tool to support experimental drop tests such as drop orientation study, parametric study and others.

Furthermore, because this is the first analysis and is exploratory in nature, technical treatment of an impact problem based on continuum mechanics is also reviewed and summarized very briefly in Appendix A. Readers who are not interested in the mathematical background and technical strategies being used may skip this part.

## 2.0 GEOMETRY OF THE CONTAINER

The configuration of the analyzed container is shown in Figure 1 (Ref. 1). It is a thick concrete tank with a lid at the top. The tank has an outside diameter of 2.6 meters. The concrete thickness for the cylindrical shell portion is 455 mm and for the bottom slab 555 mm. The outside of the container is enclosed by a 10 mm steel liner and the inside by a 15 mm liner. The lid is an inverted "hat" shaped structural component which is filled with

concrete. A 30 mm gap is filled with compressible foam material. The lid is anchored to the concrete shell using thirty-two 1 1/4" diameter ASTM A574 bolts uniformly spaced around the circumference.

## 3.0 MATERIAL PROPERTIES OF THE CONTAINER

### 3.1 Concrete

The concrete is a specially designed high density mix. Information regarding the mechanical properties of high density concrete is extremely rare and is almost nonexistent in the published literature. The only information that the writer is able to collect is the test data reported in Ref. 2. However, after comparing this data with that performed within the Ontario Hydro (Ref. 3), it is found that Ref. 2 did not achieve the same level of strength as that from Ontario Hydro tests. Test data in Ref. 2 is also judged less convincing and hence is disregarded. The final mechanical properties used in this analysis are therefore based on the Ontario Hydro test data as follows:

| | |
|---|---|
| Density | 3500 $kg/m^3$ |
| Compressive Strength | 40 MPa |
| Tensile Strength | 3.6 MPa |
| Young's Modulus | 50 GPa |
| Poission Ratio | .18 |
| Shear Modulus | 21.2 GPa |

Two types of constitutive laws are required as the concrete is to be treated as a hydrodynamic material, namely: the stress-strain relation and the equation of state. There is no constitutive data for high density concrete available from the Ontario Hydro tests. The only available information is from Ref. 2 which reported that the stress-strain relation for high density concrete is similar to that of normal weight concrete. Without further information available, the constitituve relations based on the normal weight concrete are adopted for the present analysis. They are described in the following.

#### 3.1.1 Stress-Strain Relation

The compressive stress-strain relation employed in concrete is shown in Fig. 2. Among the various proposed formulas to describe the stress-strain curve, Figure 2 was based on the CEB-FIP curve (Ref. 4) and the formulation recommended in Ref. 5 with application of the above noted property data. In general, various formulations for the curve only differ slightly and are not expected to change the response of the structure significantly. Figure 2 was later converted into a form of stress-plastic strain relation to fit the required input format in the DYNA3D computer code. It is worthwhile to mention that the increase of strength in concrete due to the increase of confined pressure (such as the Mohr-Coulomb failure law) is not applied to this particular exercise. Concrete is considered to have lost its entire strength after crush as shown in the figure.

When the stress is in tension, the relation is controlled by the Young's modulus and the tensile strength specified above. There is no tension stiffening nor shear retention considered in the computer code and hence the analytical results would be on the conservative side.

The reinforcement in the concrete is not included in the current analysis. Reinforcement plays a less important role under the current drop orientation. It is therefore decided to keep the analysis simple but conservative.

### 3.1.2 Equation of State

In general the equation of state for a material relates hydrostatic pressure P to the volume change (or density change) and to the internal energy. In this analysis the pressure is assumed to be only dependent on the former as shown in Fig. 3. The figure indicates that for a concrete cube subjected to a pressure, the pressure initially increases proportionally to the decrease of volume (or increase of density) until the concrete collapses (crushing) at point A. The proportionality (i.e., the slope of line OA) is the bulk modulus of concrete. After collapse, the concrete engages in a compacting stage (line AB) with less pressure required for further volume decrease until the full compaction is achieved at point B. Thereafter the concrete regains approximately its original bulk modulus for further compression (line BC). If the pressure is released after concrete collapse such as at point E, elastic unloading should occur with a permanant volume change.

If the concrete is subjected to tension, the required negative pressure to increase the volume is similar to that of compression with the same bulk modulus. This continues until the maximum tensile strength of the concrete as represented by the spall limit $P_{min}$ is reached and then the concrete starts to crack and pressure is dropped to zero.

In the current analysis this pressure-volume change curve is approximated by three pieces of linear lines where point A and B represent the points of intersection. The values of these parameters used in the analysis are:

| | |
|---|---|
| Bulk Modulus | $K$ = 26 Gpa |
| Bulk Modulus for compacting state | $K_c$ = 13 Gpa |
| Pressure at point A | $P_A$ = 160 MPa |
| Pressure at point B | $P_B$ = 3000 MPa |
| Volumetric strain at point A | $\epsilon_A$ = 0.006 |
| Volumetric strain at point B | $\epsilon_B$ = 0.24 |

## 3.2 Steel Liner

The material for both outer and inner liners is G40.21M 300WT steel to ensure its energy absorption capability being conserved under cold temperature. Its mechanical properties are as follows:

| | |
|---|---|
| Density | 7850 kg/m |
| Young's Modulus | 200 GPa |
| Poision Ratio | 0.3 |
| Yield Strength | 300 MPa |

For its stress-strain relation, the steel is treated as elastic - perfectly plastic as shown in Fig. 4. The minimum guaranteed yield strength in accordance with the CSA Standard for structural steel is employed. In the analysis a negligible amount of strain hardening is introduced to avoid any possible numerical instability at the perfect plastic stage. Essentially the additional strength due to strain hardening is ignored.

## 4.0 FINITE ELEMENT MODELING OF THE CONTAINER

The container is transformed into a mathematical model through the interactive engineering software PATRAN. As the finite element technique will be applied in the analysis, the concrete is simulated by solid elements and the steel liners by shell elements. PATRAN, functioning as a pre-processor, creates these elements and generates a set of input data for later analysis. Due to its symmetry, only half of the container and payload mass of 8,640 kg are modelled.

The finite element mesh for each component are illustrated in Fig. 5, 6, 7, 8, and 9 for the outer liner, inner liner, lid plate, lid in-filled concrete and container concrete respectively. The impact regions are modelled by a refined mesh in order to obtain more accurate results at that area. The refinement is gradually reduced for the region further away from impact location for economy of computing cost. The pattern of the mesh generated for the concrete is identical to that of the steel liners while the concrete is divided into four layers of solid elements though the thickness. Figure 10 shows the cylindrical cask concrete in colour-filled solid form. Figure 11 provides a complete picture of the lid including the shell elements for steel plates (in black) and the solid elements for concrete (in blue). Note that a 30 mm gap between the concrete and the lid cover plate is modelled to reflect the physical configuration of the lid while the stiffness of the filled compressible foam material is judged negligible and is ignored. Figure 12 constitutes the entire CIC where a 20 mm gap between the lid and the inner liner is provided as per the cask design (Ref. 1). The lid is rigidly connected to the cylindrical portion of the cask only along the circumference with anchor bolts. Small holes were created through the lid slab and the container slab to avoid using triangular elements and hence eliminates the possibility of generating unreasonable stress due to acute triangle elements. Figure 13 shows the complete finite element model of the system including the container and the rigid surface. The rigid surface is modelled as solid elements and is restrained from movement.

## 5.0 ANALYTICAL RESULTS AND DISCUSSIONS

The container, without an impact limiter for protection, is assumed to undergo a nine (9) meter upside down free drop with its corner edge impacting onto a rigid ground. The formal stress analysis is carried out using the hydrodynamic code DYNA3D, an explicit three dimensional finite element code for analyzing the large deformation dynamic response of inelastic solids and structures. The analytical data is then fed back to PATRAN for post-processing. With its color graphic capability, PATRAN sorts, interprets, summarizes and presents the resulting data as follows:

Figure 14 is a normalized momentum time history plot of the container. It indicates that the container reaches a full stop at approximately 0.05 seconds after initial impact. The same result is shown in Figure 15 for the kinetic energy time history of the container. In fact the container gradually picks up kinetic energy again after 0.05 seconds indicating a rebound.

Figure 16 provides the velocity time history at the tip of the container (also the tip of outer liner) which is the first contact point when the container impacts onto the surface. The velocity fluctuates at the beginning due to numerical noise but quickly stabilized to zero which means that the tip physically remains in contact with the rigid surface. It is noticeable that the velocity starts to increase in the positive direction (i.e. physically upward) after 0.05 seconds which implies a rebound of the tip point. A similar response of the tip point is seen in Figure 17 in terms of displacement. Note that the displacement in the plot is in units of one tenth of a millimeter and is very small. Again it indicates numerical noise at the beginning, stabilizes to zero displacement and later starts to rebound after the full stop. Figures 18 and 19 demonstrate the corresponding velocity and displacement time history at the tip of inner liner respectively. Again the velocity decreases from the initial velocity to zero and then tends to increase in the positive direction indicating a rebound. The displacement plot indicates that the tip moves downward and eventually hits the target pad.

Figure 20 shows the total contact force (i.e. impact force) between the container and the rigid surface through the entire impact. It can be seen that the maximum impact force is reached at approximately 0.027 seconds and lasts until about 0.042 seconds before it starts to decline again (i.e. the container starts to disengage from the rigid surface). The peak force is close to 13 MN while the average is approximately 12 MN. These are correspondingly 38 and 36.5 times the CIC weight (i.e. 38g and 36.5g respectively).

Deformation of the container is shown in Figures 21 and 22. Figure 21 demonstrates the deformation of the outer liner while Figure 22 shows the inner liner. It can be seen that the outer liner deformed significantly while the inner liner deformed mildly at the bottom edge only. Figure 23 is a larger scale plot of the bottom portion of the outer liner. The black indicates an "elephant foot" shape deformation at impact while the blue background represents the original undeformed shape. Similarly, Figure 24 demonstrates the deformation at the tip of inner liner.

Stresses and strains are examined at 0.032 seconds and 0.04 seconds which correspond to the early stage and end of the maximum impact force period. It is found that stresses and strains at 0.032 seconds are slightly less than that at 0.04 seconds and hence only the later are reported and discussed herein. Stresses and strains are reduced after 0.04 seconds due to elastic unloading.

Figures 25, 26 and 27 are the Von Mises stress contour plots at the inner, middle and outer surfaces of the outer liner respectively. The difference between the middle surface and inner/outer surfaces plots is that the former

represents the in-plane stress while the latter is the sum due to in-plane and bending. Recalling that the yield strength of the liners is 300 MPa, the portion of the liner in red has stresses at or close to yield. Note that the tip (i.e. the initial impact area) may not be subjected to the maximum stress at this stage since it has already buckled. As the contact area grows larger, the indented tip which initially yielded has already experienced unloading. Stress has subsequently been redistributed toward the outer circumferential region as shown in the figures. Further away, the stress starts to decrease which means that the remaining portion of the outer liner maintains elastic throughout the impact.

Similar structural response of the outer liner is demonstrated in terms of the equivalent plastic strain contour plots at the inner, middle and outer surfaces in Figs. 28, 29 and 30 respectively. The strain level suggests that the outer liner may be subjected to a ductile fracture failure at its most bulged region.

Similarly Figures 31, 32, 33 and 34 are the Von Mises stress and equivalent plastic strain contour plots at the middle and outer surface of the inner liner. It can be seen that the response of the inner liner is similar to that of the outer liner except that both stress and strain levels are much lower.

Figure 35 is a Von Mises stress contour plot for concrete. The impact corner in white represents the range of concrete being crushed. As the concrete is crushed, it is not capable of carrying shear stress and hence the Von Mises stress becomes zero. The pulverized concrete transmits further stress to the unfailed concrete through direct stresses (i.e. pressure).

Figure 36 is the stress contour plot for the steel plates of the lid. Note that localized yielding occurs at the "web" immediately above the junction of the web and horizontal plate near the impact location (see the red in the figure). This is understandable from a structural point of view since this area is physically the weakest spot under the current drop orientation. It is interesting to observe that the stress is passed through the stiffened web-horizontal plate junction path and redistributed toward the far end of the lid. However these stresses are below yield and the plates remain elastic.

## 6.0 CONCLUSIONS

A stress analysis of the concrete integrated container impacting onto a rigid surface has been demonstrated. The analysis enables the response of the container in terms of various parameters at different stages of the impact to be studied in detail. This is vital information for the design of the container.

The analysis is conservative because the concrete reinforcements, the additional strength of the steel liners due to strain hardening and the increase in concrete strength due to confined pressure are all not considered. The extent of damage predicted from this exercise can therefore be viewed as the worst possible situation. It is noted that the damage to the outer liner and the concrete are localized in the vicinity of the impact area. The inner liner experiences less damage. However this analysis does indicate that an

impact limiter is a necessity in order to ensure the complete structural integrity of the container. It is judged that an impact limiter composed of effective energy absorption material will eventually eliminate any possible damage in the container itself.

## 7.0 FUTURE WORK

The analytical work under the CIC project includes the following four parts:

1. A demonstrative analysis to explore the feasibility of using the theoretical approach to investigate the CIC,
2. Validation analyses to simulate the drop tests and compare the results,
3. Drop orientation analyses to study the damage on the CIC due to different impact orientations,
4. Full scale impact analyses based on the final design of the CIC and impact limiter.

This report covers Part 1 of the above mentioned work. The remaining work will be reported in the near future upon the completion of each part.

Approved by:

G.J. Clarke
Manager
Mechanical Research Dept.

Submitted by:

H.P. (Jack) Lee
Engineer
Applied Mechanics Section

Recommended by:

J.A. Chadha
Supervising Engineer
Applied Mechanics Section

Reviewed by:

T.P. Byrne
Unit Head-Stress Analysis & Heat Transfer
Applied Mechanics Section

HPL:cm

## REFERENCES


(1) Irradiated Fuel Storage Program, Concrete Integrated Cask Conceptual Design, Ontario Hydro Drawing No. 0973-DOH-03760-0010, Nov. 27, 1986.

(2) Raju, N. Krishna, "Properties of High Density Concrete", Indian Concrete Journal, May 1984, p. 130-133.

(3) Hooton, R.D., "Development of High Strength, High Density Concrete Mixes", Ontario Hydro Research Report No. 85-132-H, June 1985.

(4) Comité Euro-International du Béton/Fédération Internationale de la Précontrainte, "CEB-FIP Model Code for Concrete Structures", 3rd ed., Paris, 1978.

(5) Chen, W.F., "Plasticity in Reinforced Concrete", McGraw-Hill Inc., 1982.

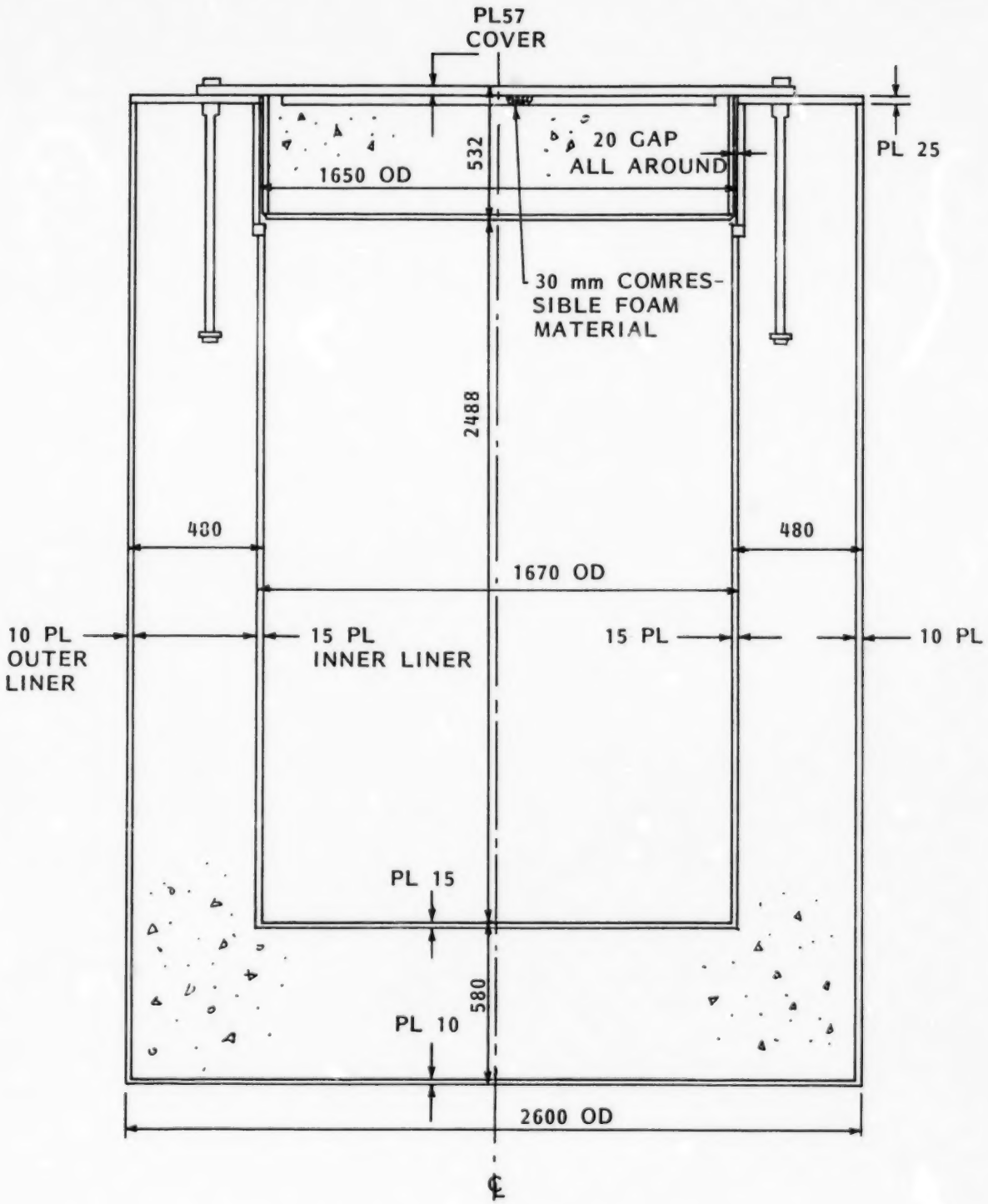


Fig. 1 CONCRETE INTEGRATED CASK
(SECTION VIEW)

89-286

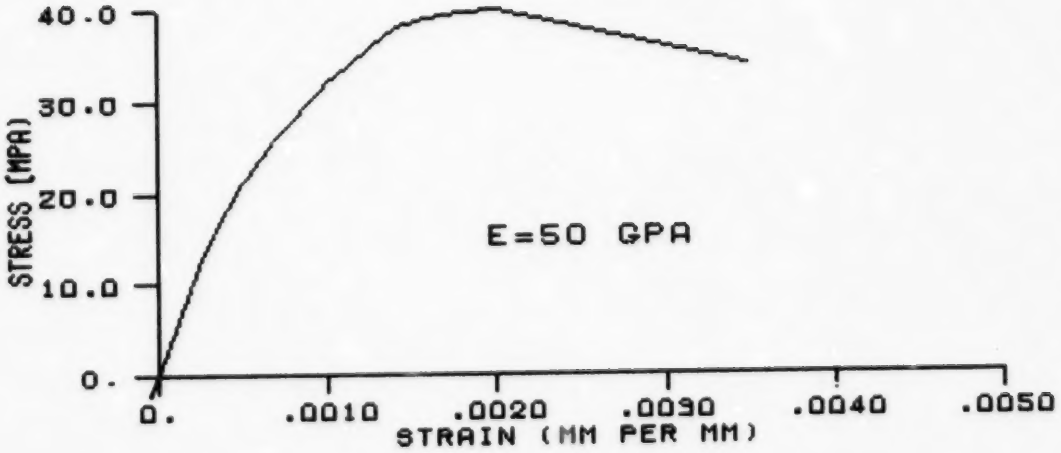


(IN COMPRESSION)

FIG. 2 STRESS-STRAIN CURVE FOR THE CONCRETE

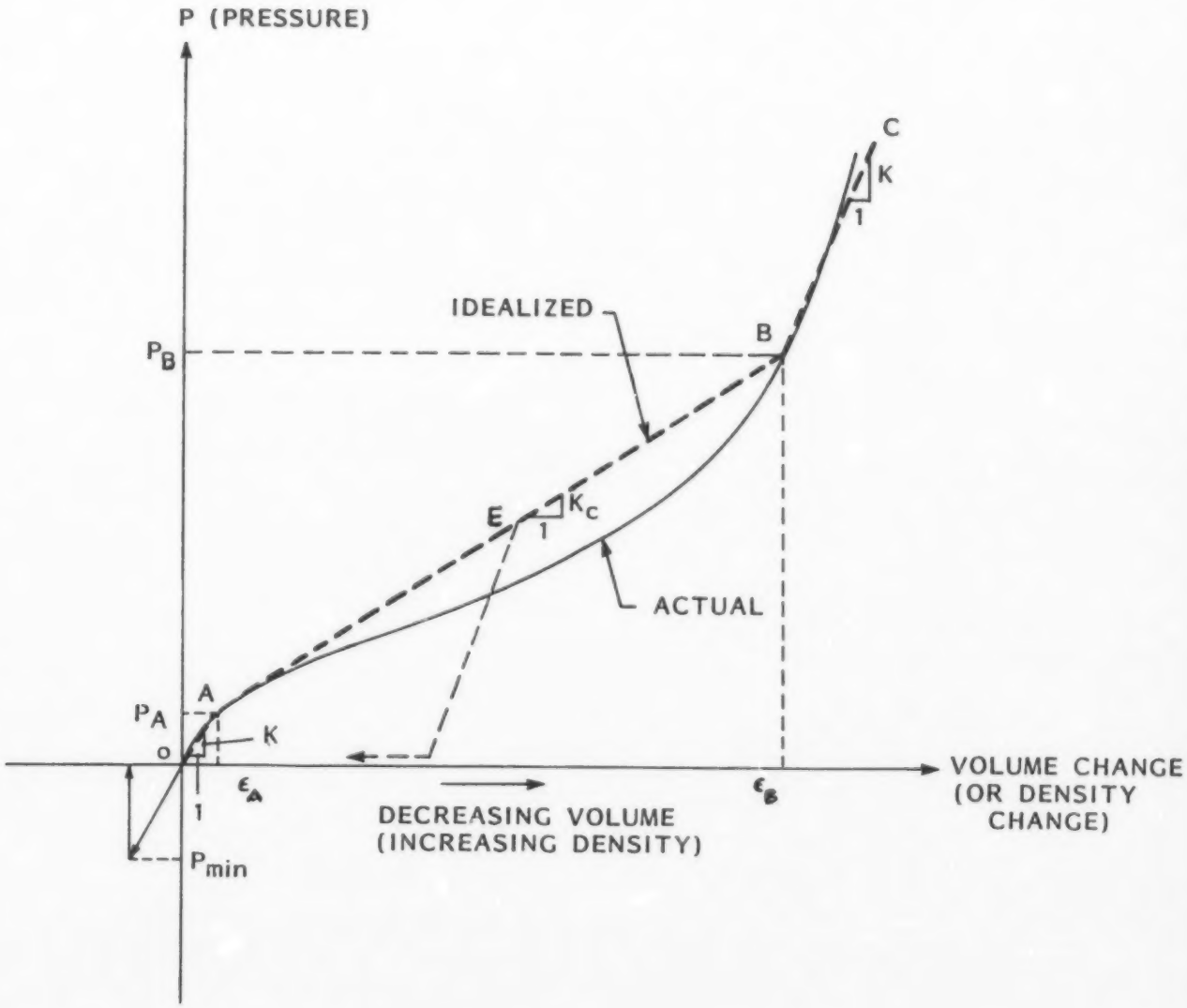


FIG. 3 EQUATION-OF-STATE MODEL FOR CONCRETE

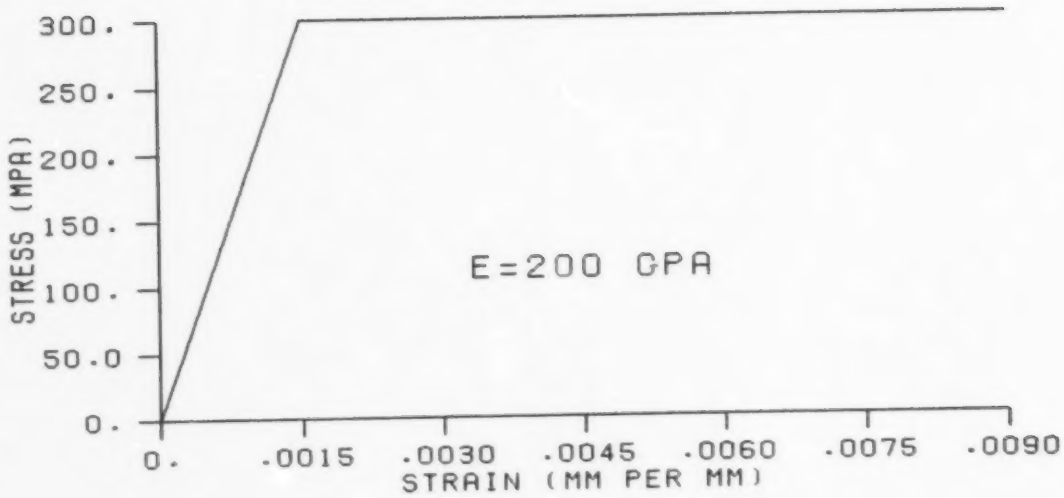


FIG. 4 STRESS-STRAIN CURVE FOR THE LINERS

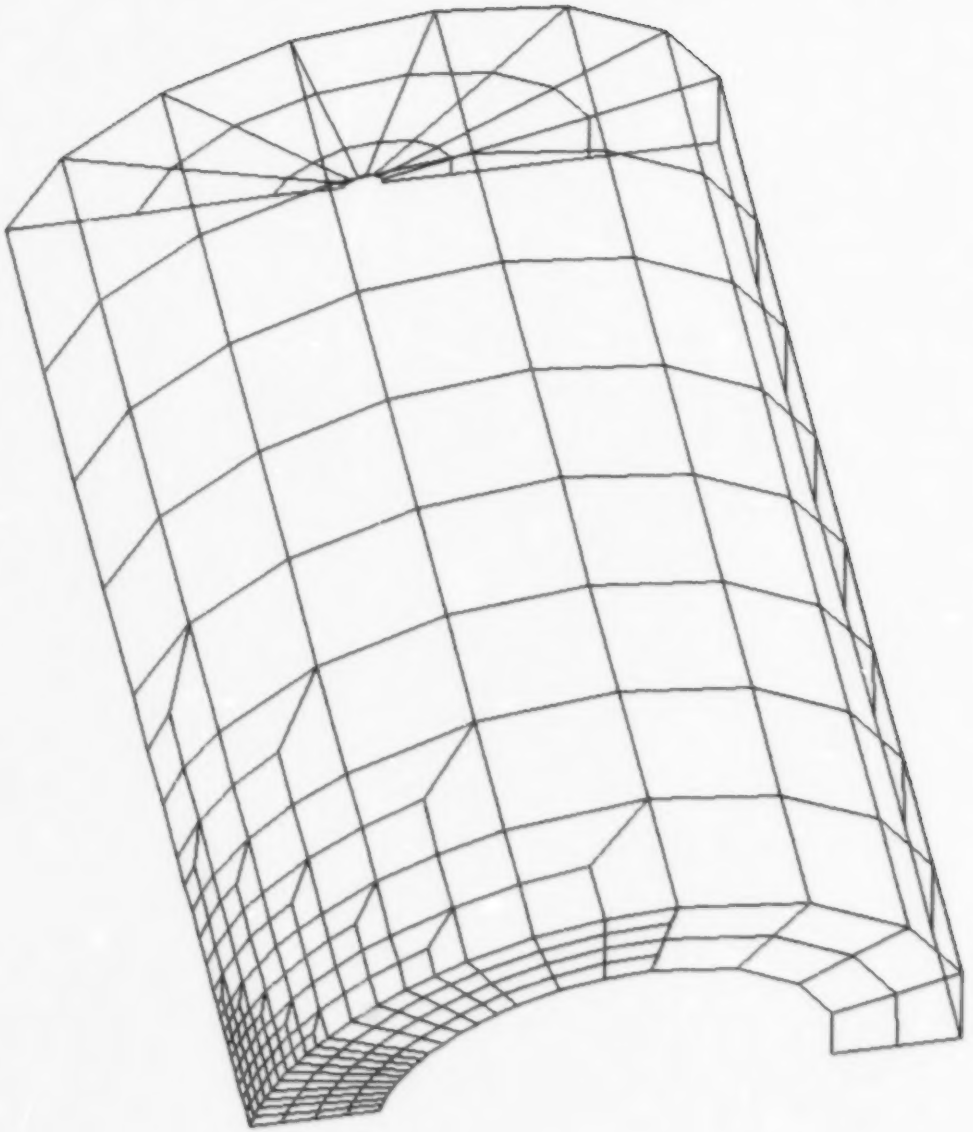


FIG. 5 SHELL ELEMENTS FOR OUTER LINER



99-366

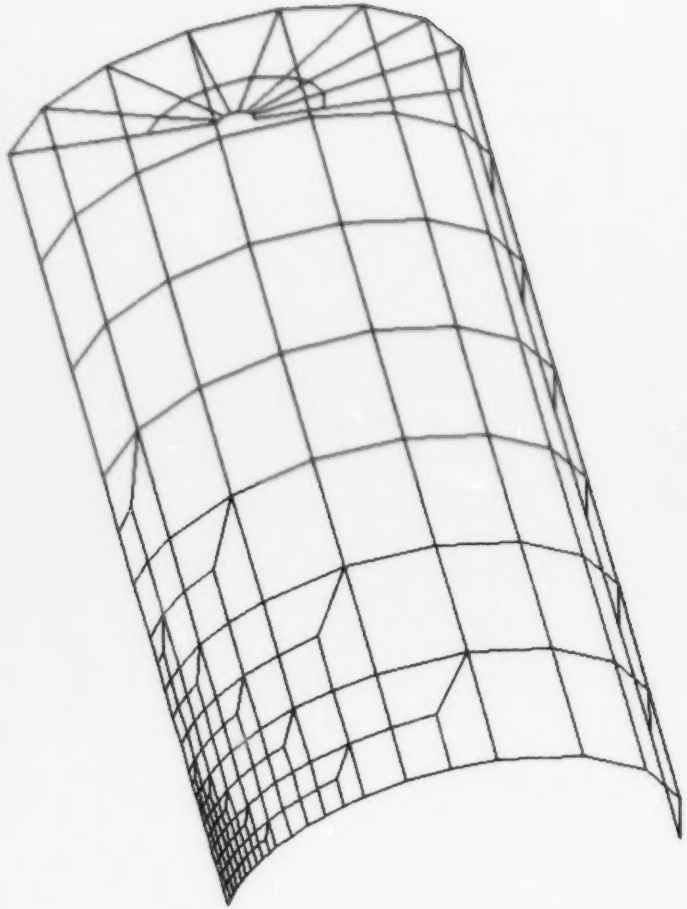


FIG. 6 SHELL ELEMENTS FOR INNER LINER

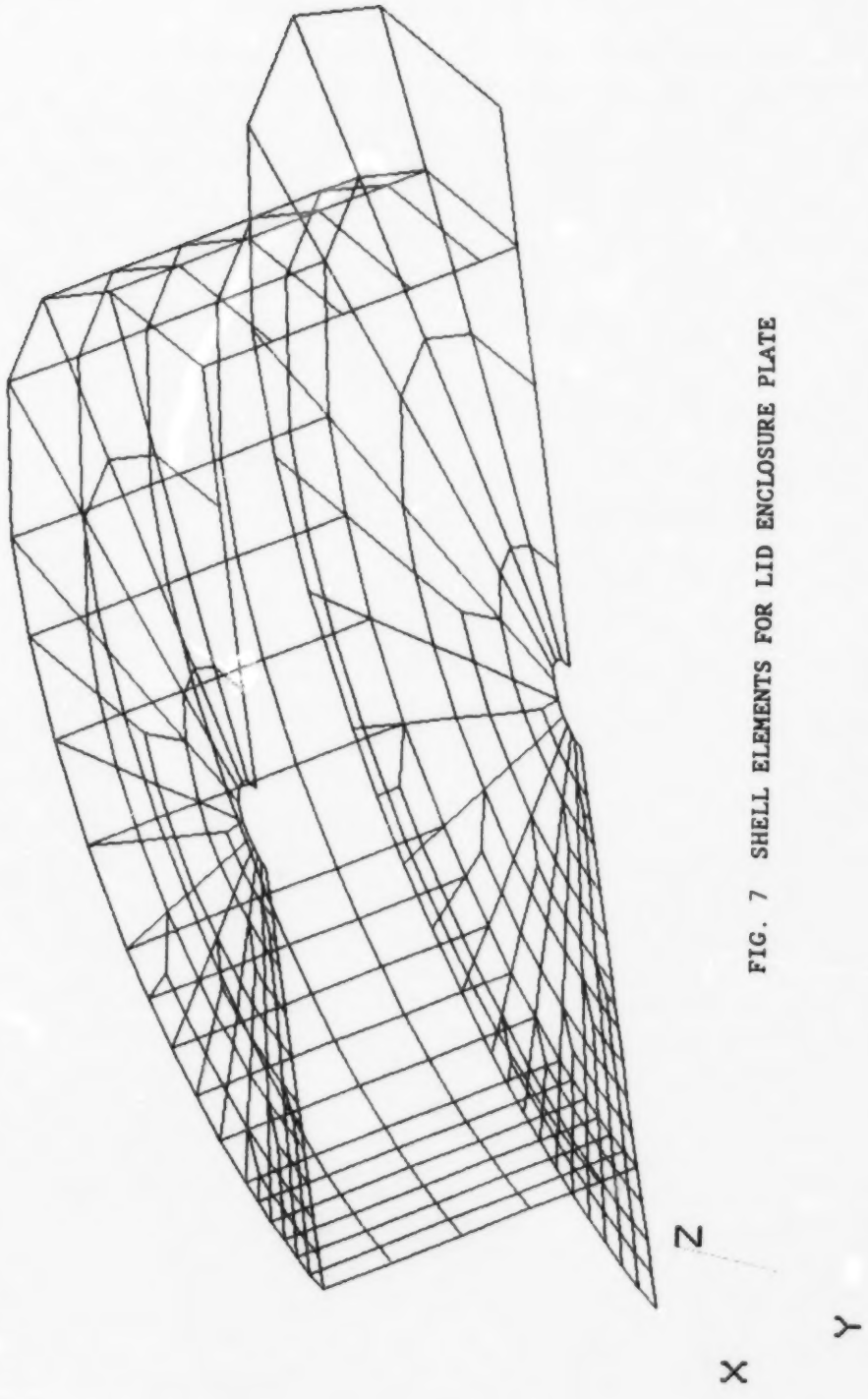


FIG. 7 SHELL ELEMENTS FOR LID ENCLOSURE PLATE

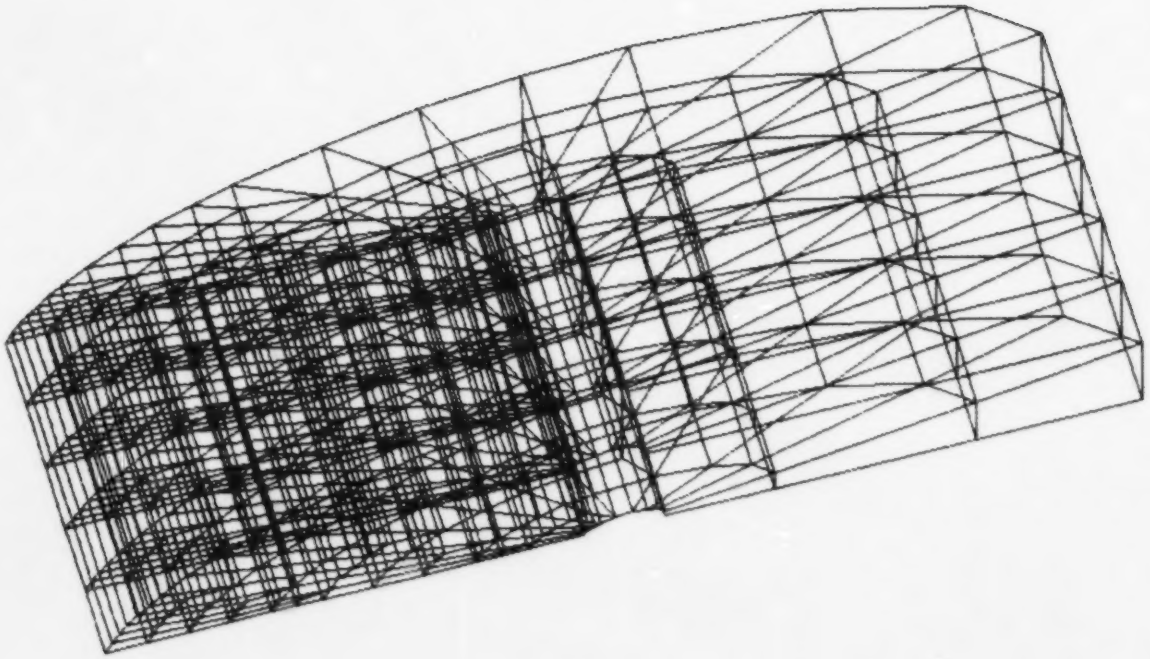

FIG. 8 SOLID ELEMENTS FOR LID CONCRETE

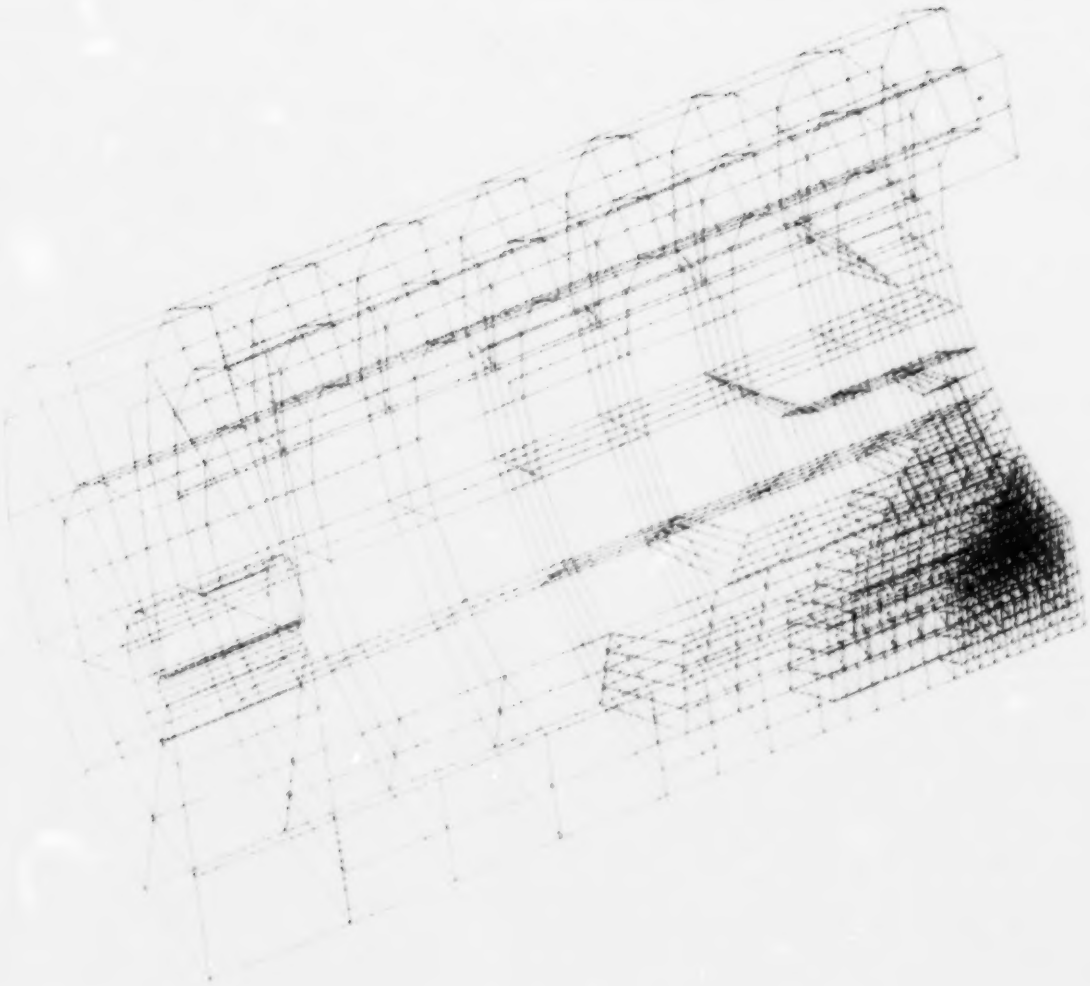


FIG. 9 SOLID ELEMENTS FOR CONTAINER CONCRETE



83-286

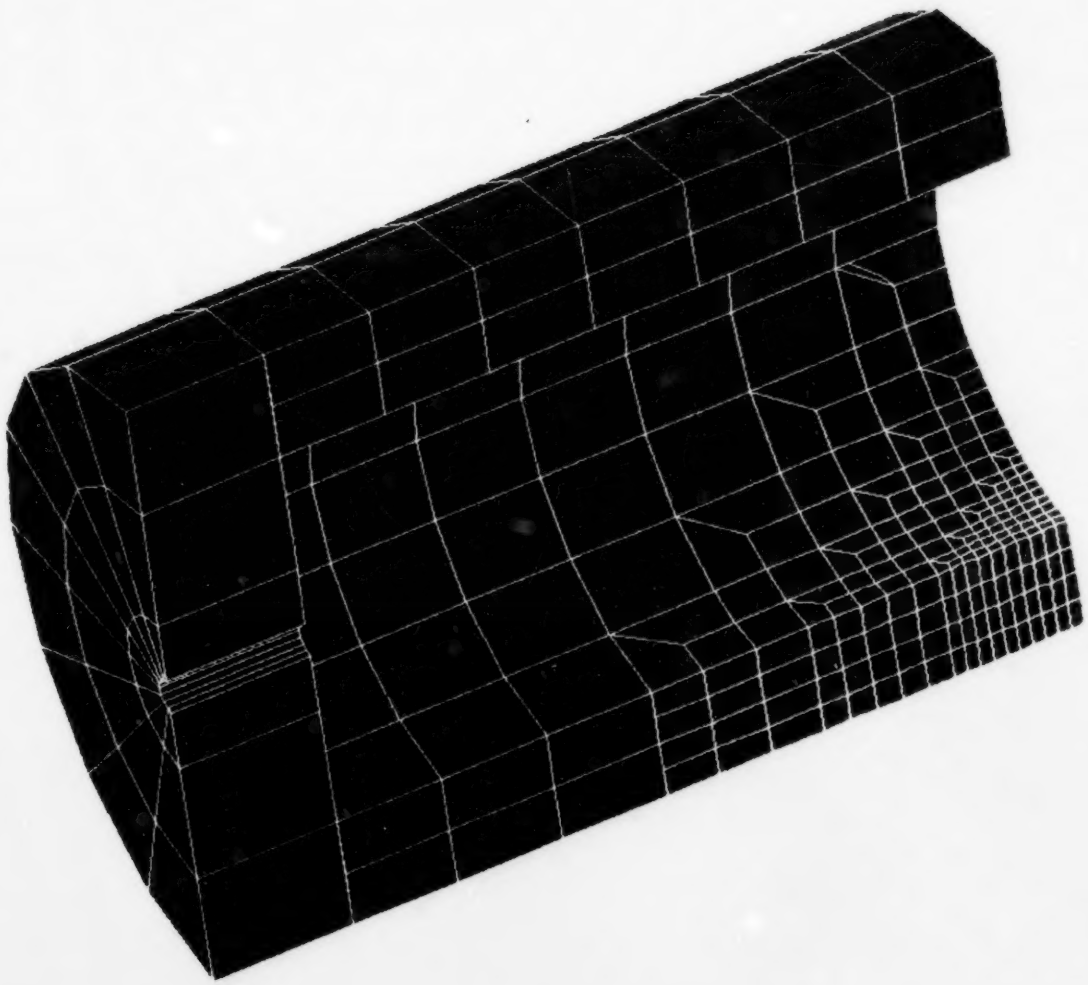


FIG. 10 SOLID ELEMENTS FOR CONTAINER CONCRETE



89-286

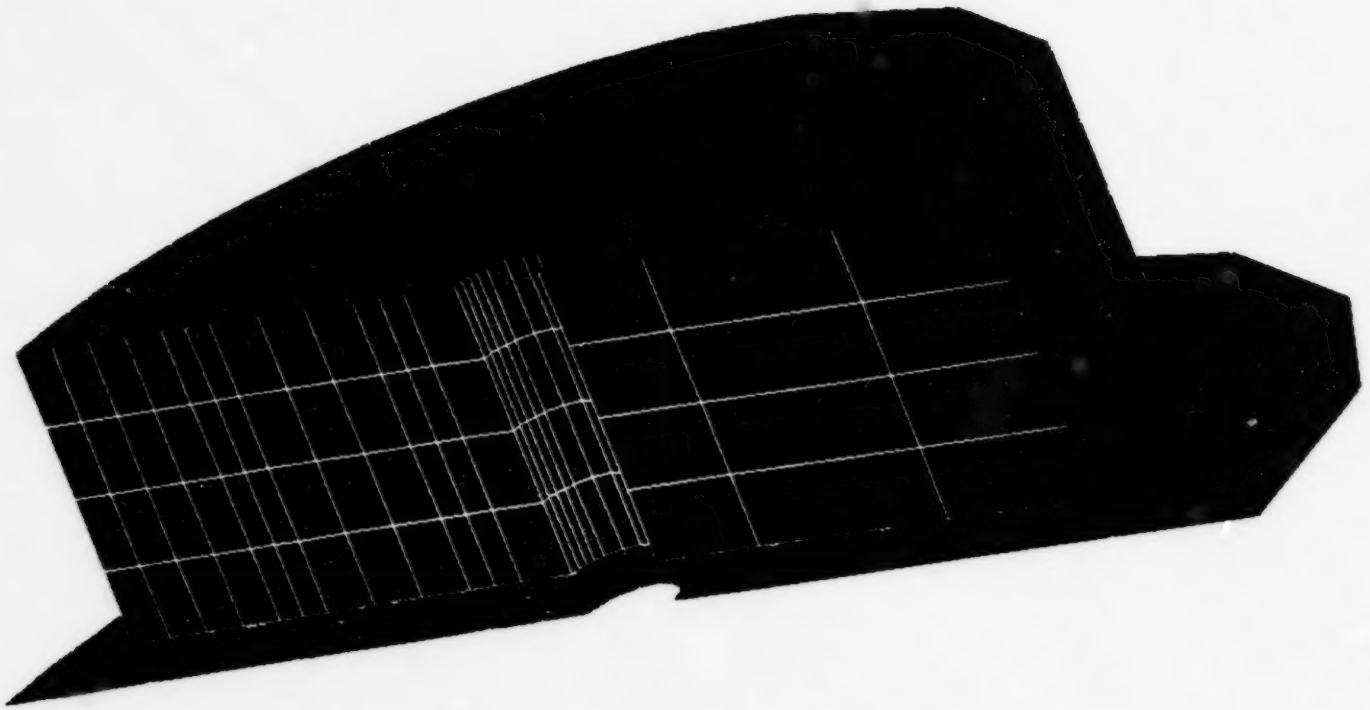


FIG. 11 COMPLETE FINITE ELEMENTS FOR LID

FIG. 12 COMPLETE FINITE ELEMENTS FOR CIC



89-286

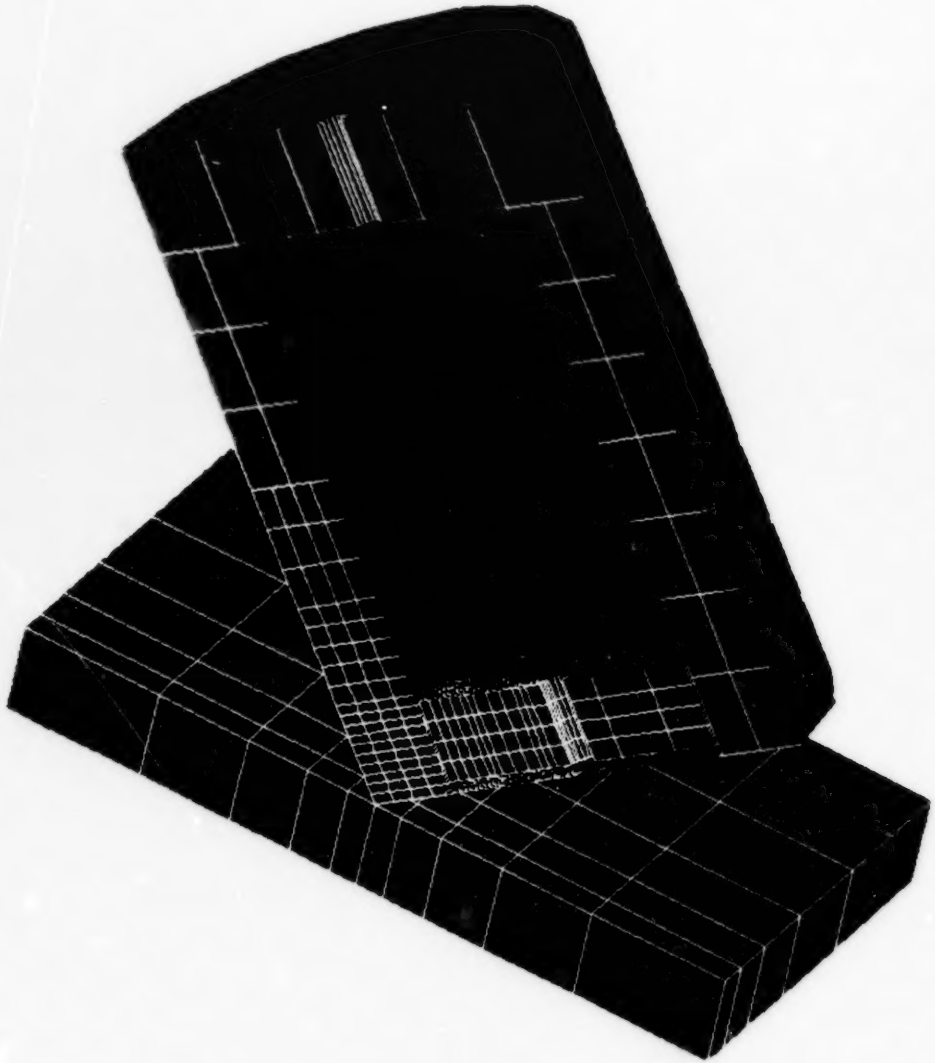


FIG. 13 COMPLETE FINITE ELEMENT MODEL OF THE SYSTEM

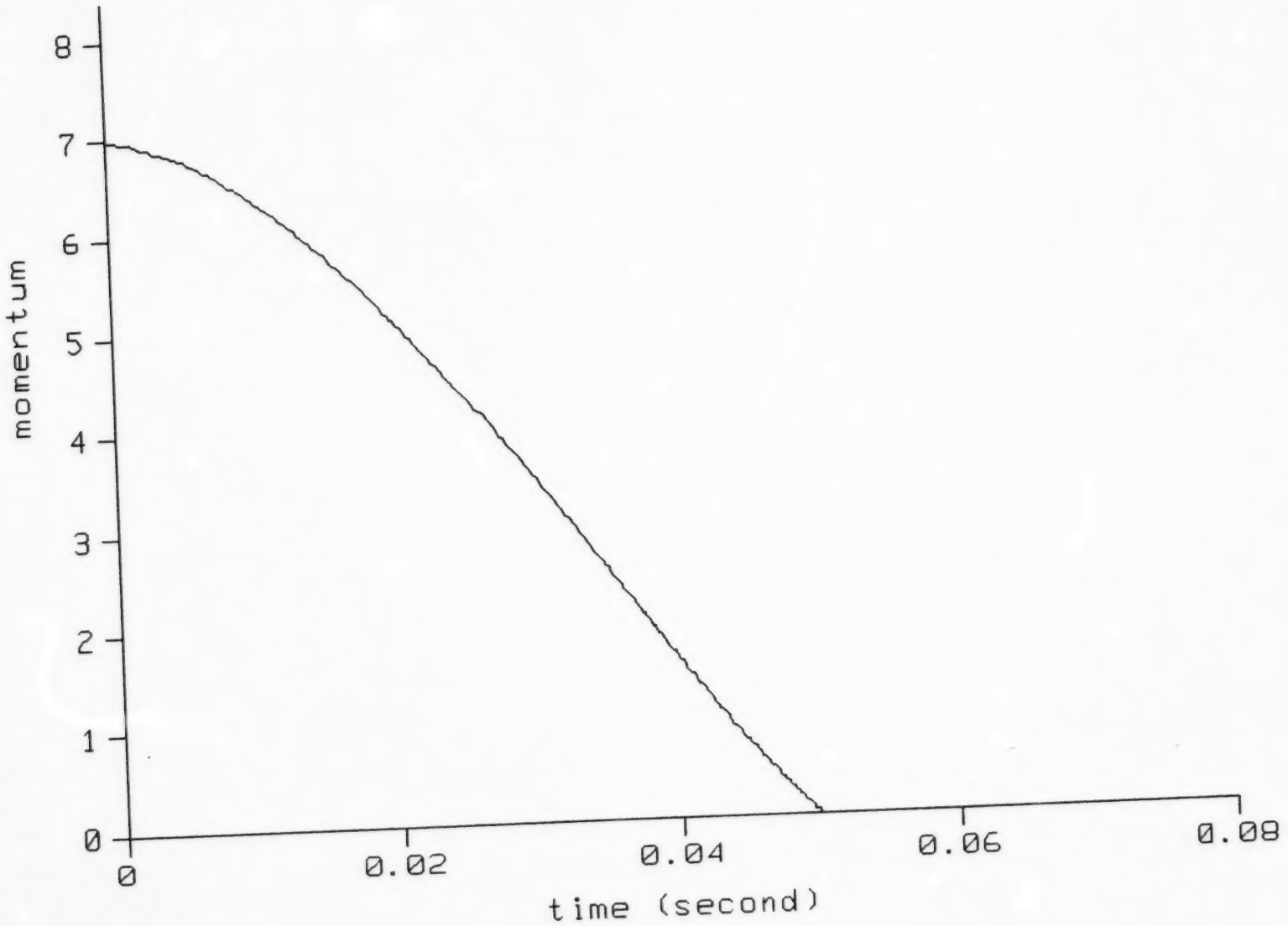


FIG. 14 NORMALIZED MOMENTUM TIME HISTORY OF CIC

89-286

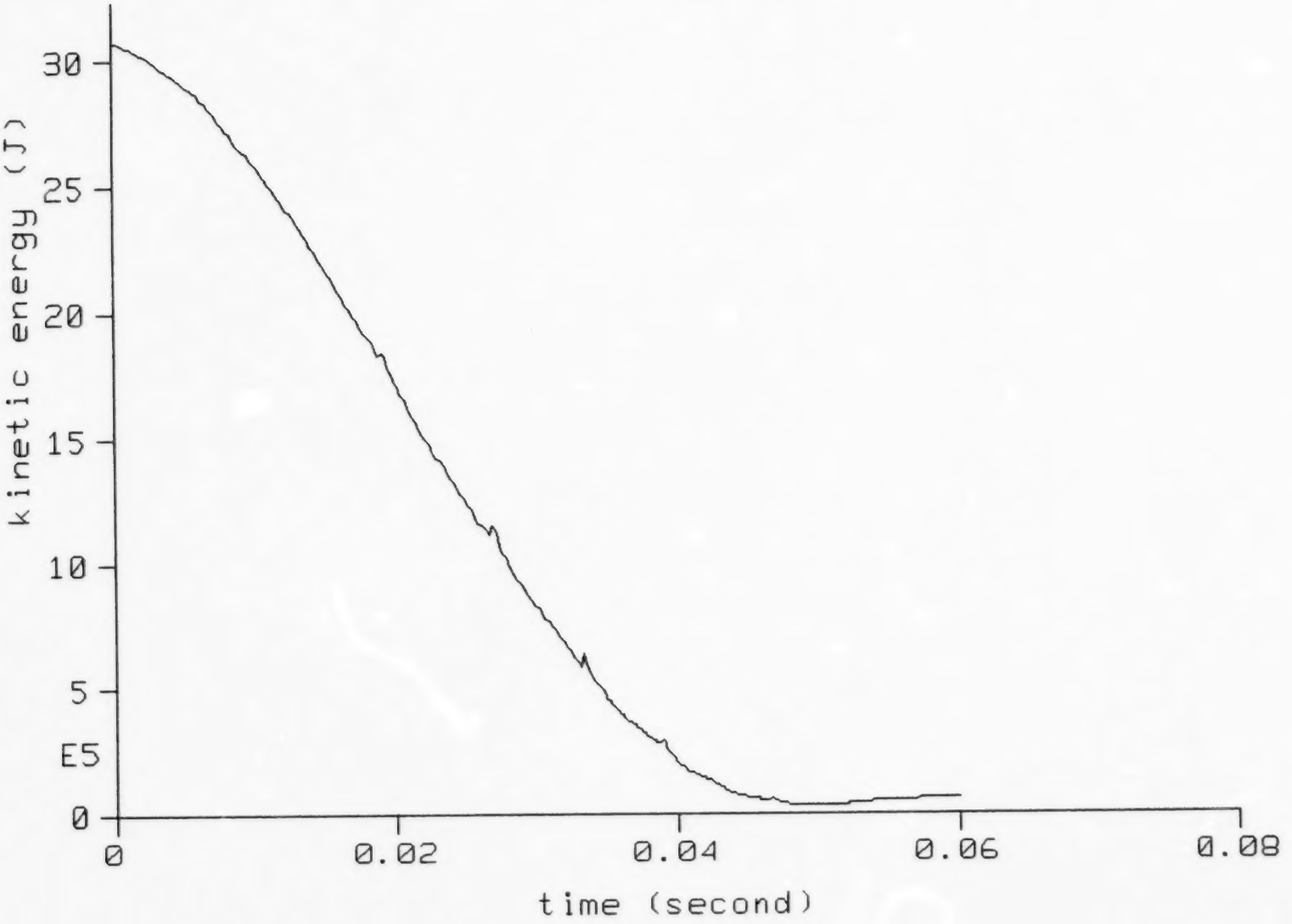


FIG. 15 KINETIC ENERGY TIME HISTORY OF CIC

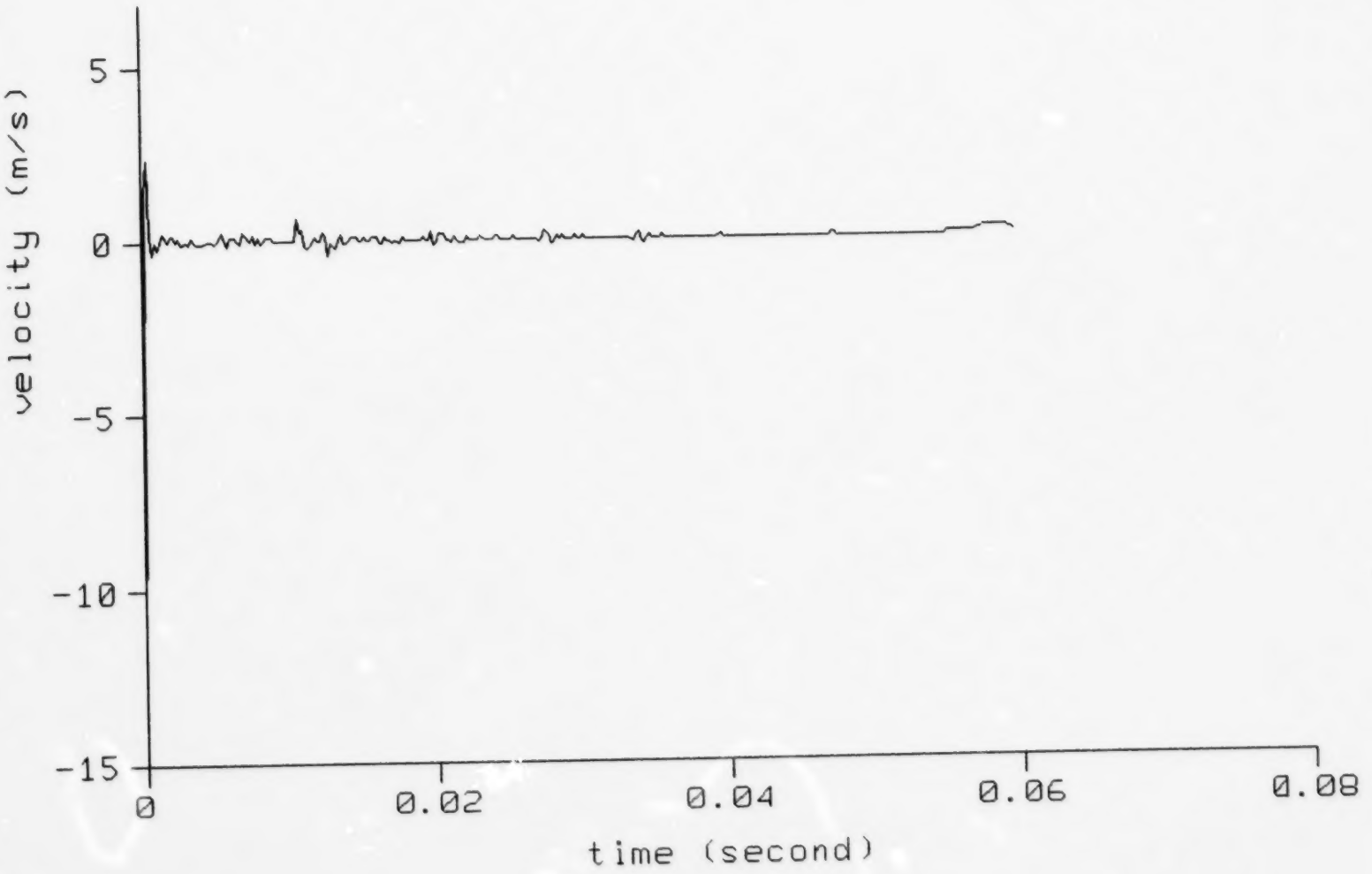


FIG. 16 TIME HISTORY OF VELOCITY AT TIP OF CIC

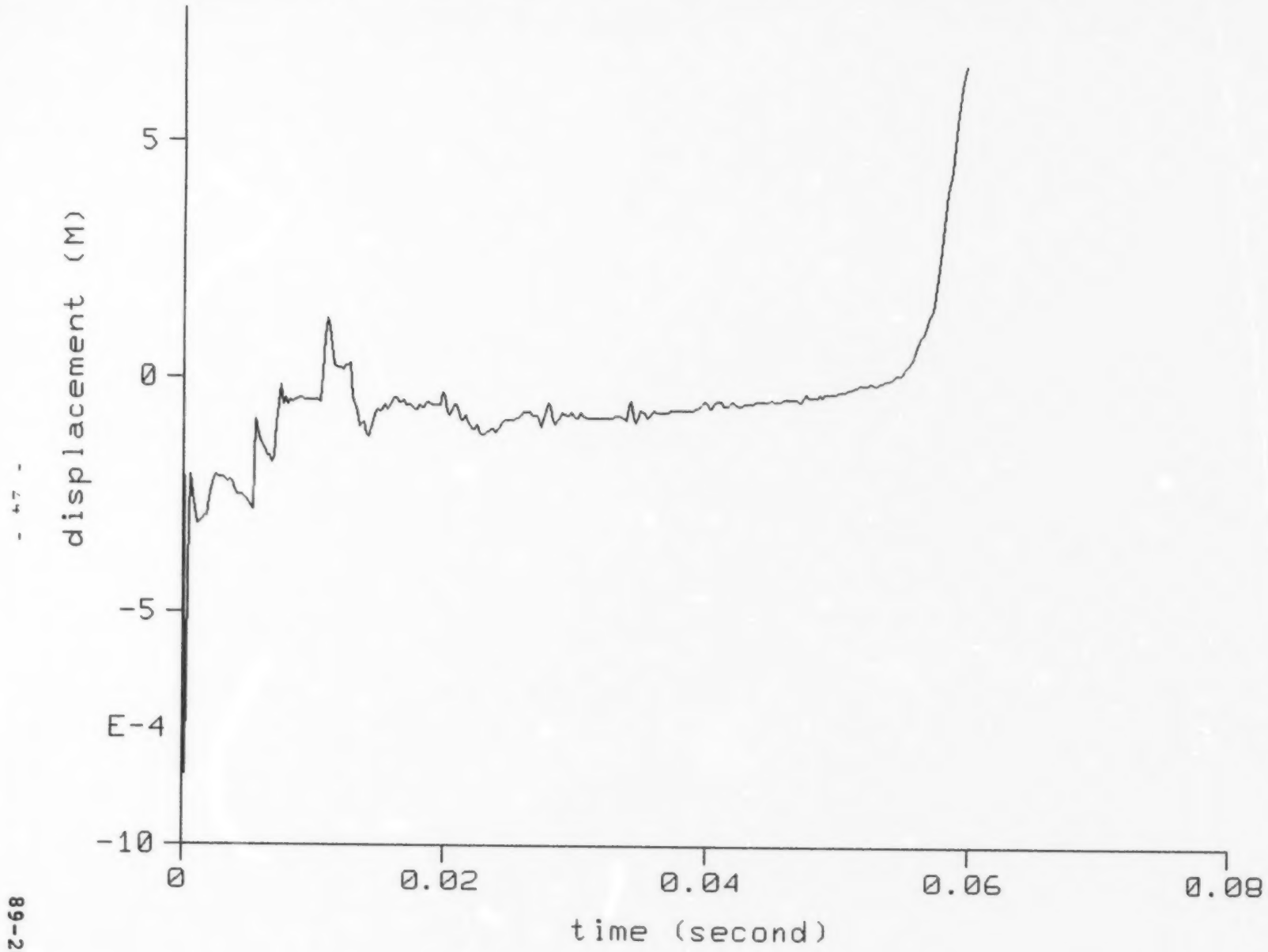


FIG. 17 TIME HISTORY OF DISPLACEMENT AT TIP OF CIC

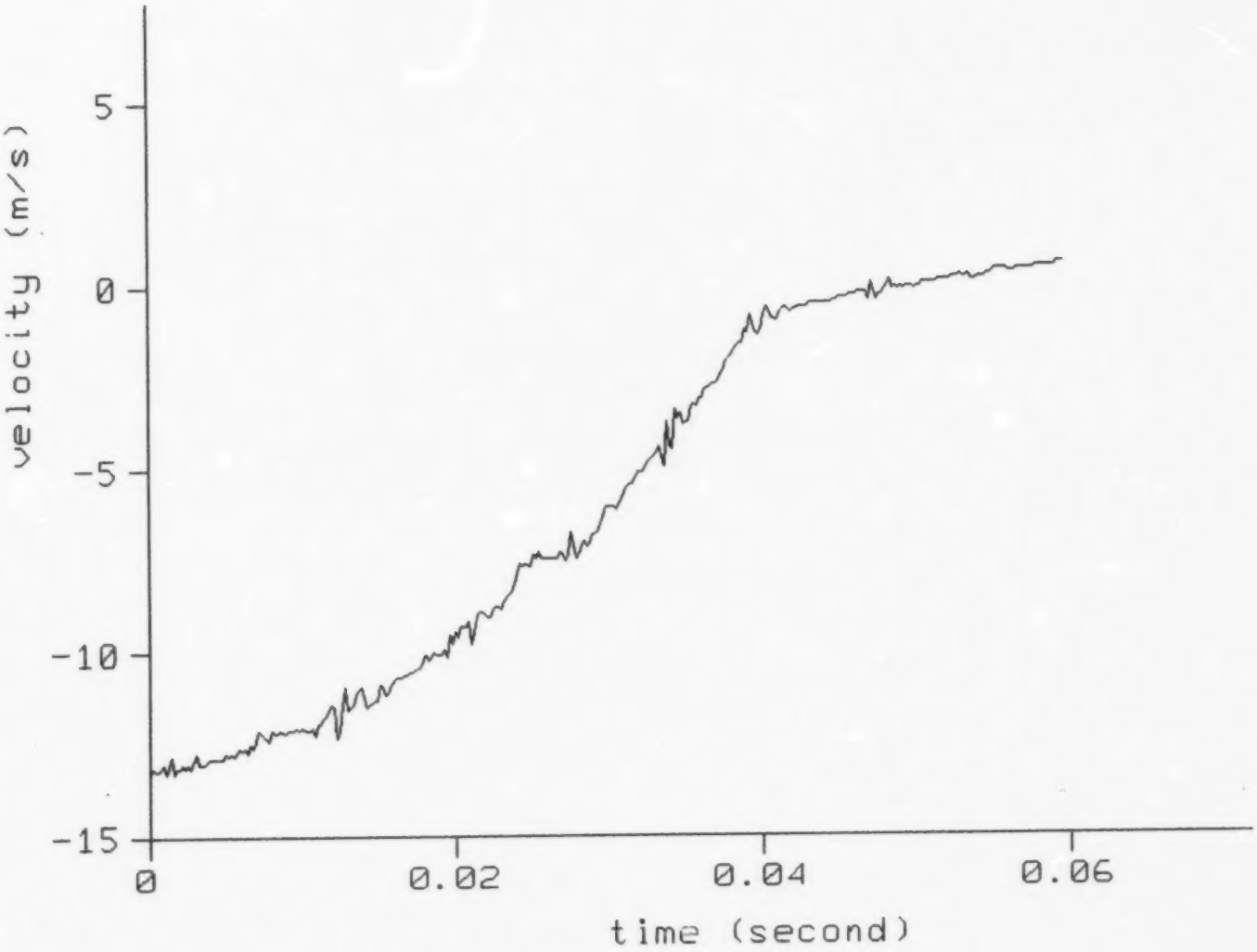


FIG. 18 TIME HISTORY OF VELOCITY AT TIP OF INNER LINER

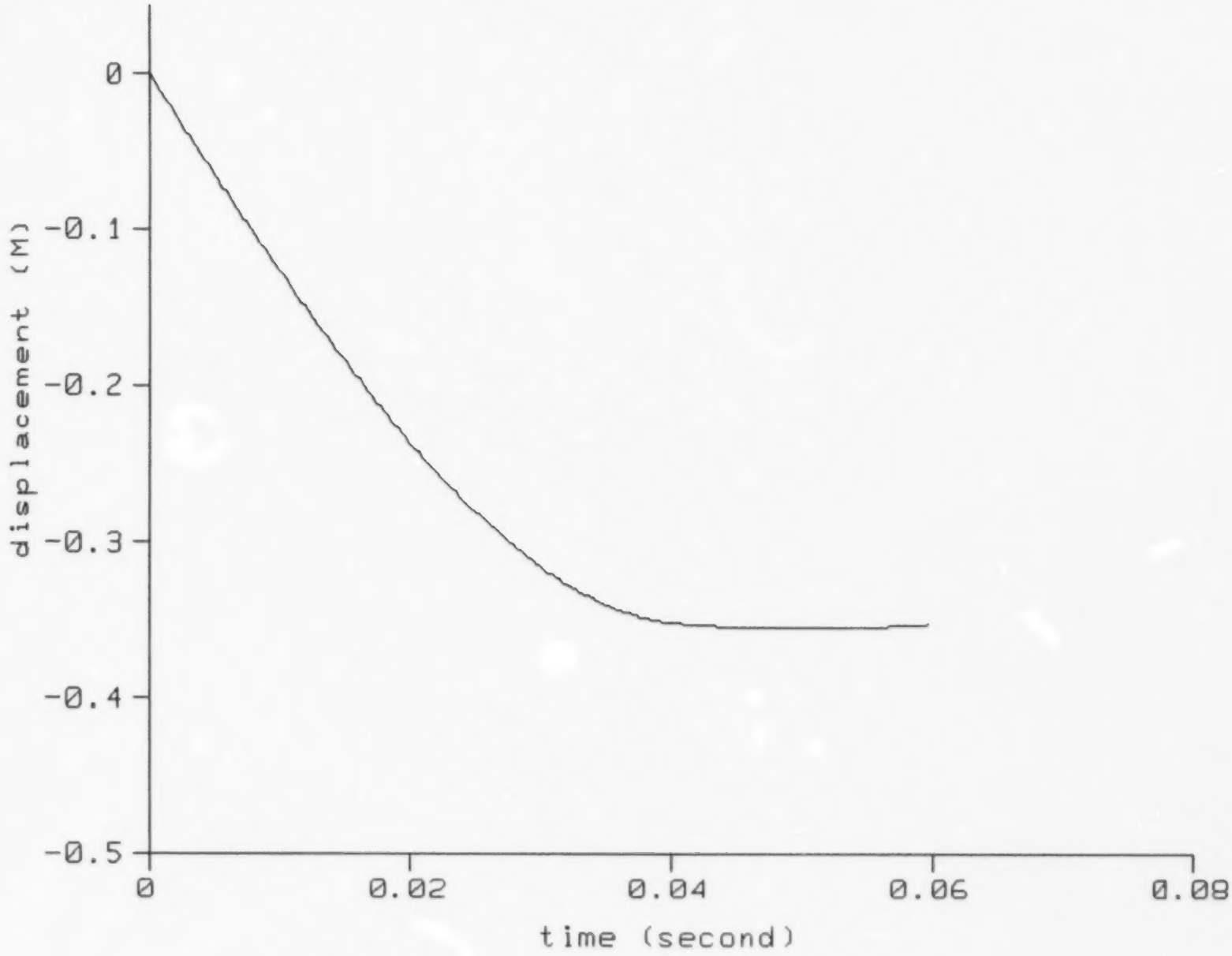




aa-286

FIG. 19 TIME HISTORY OF DISPLACEMENT AT TIP OF INNER LINER

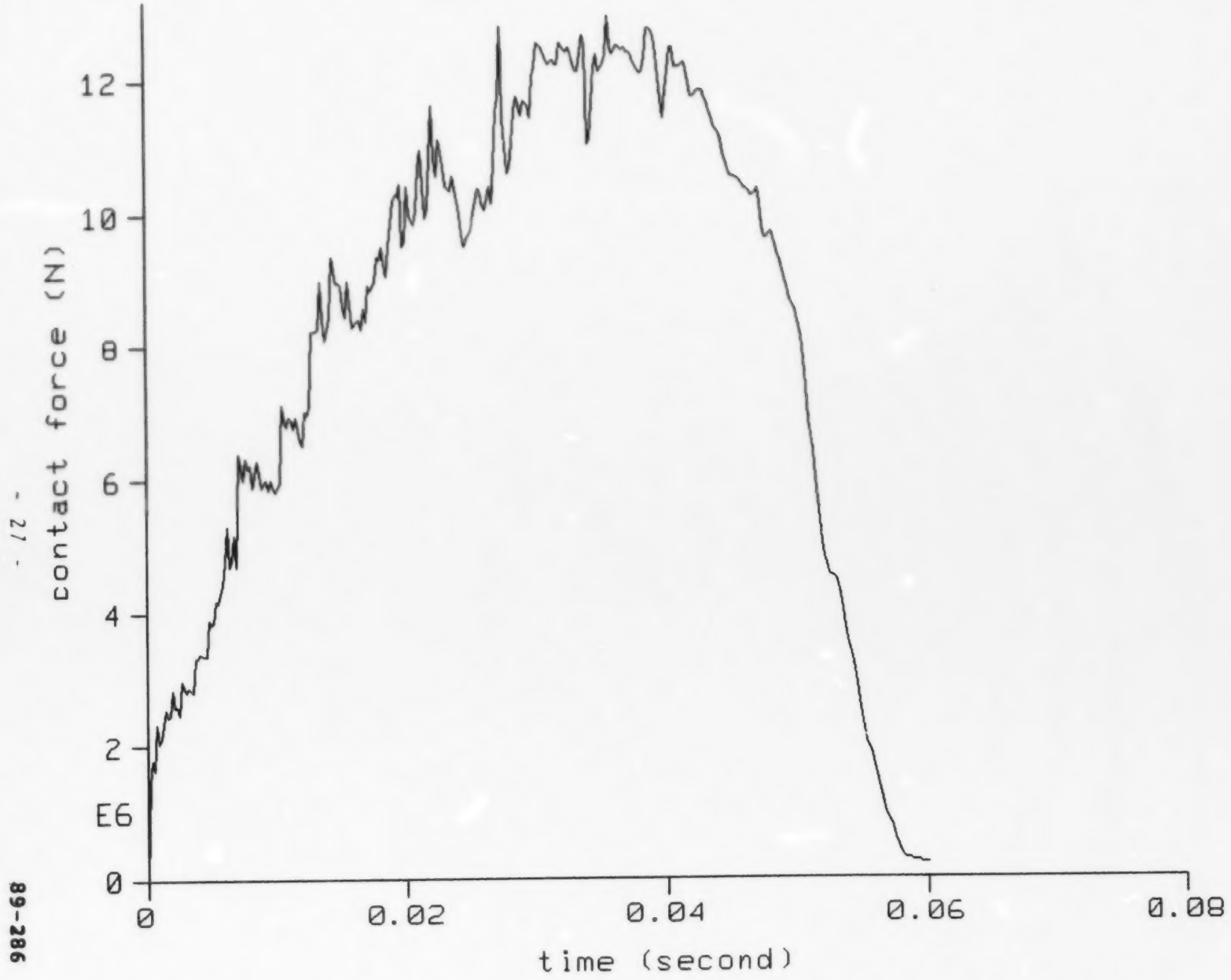




FIG. 20 CONTACT FORCE TIME HISTORY OF CIC

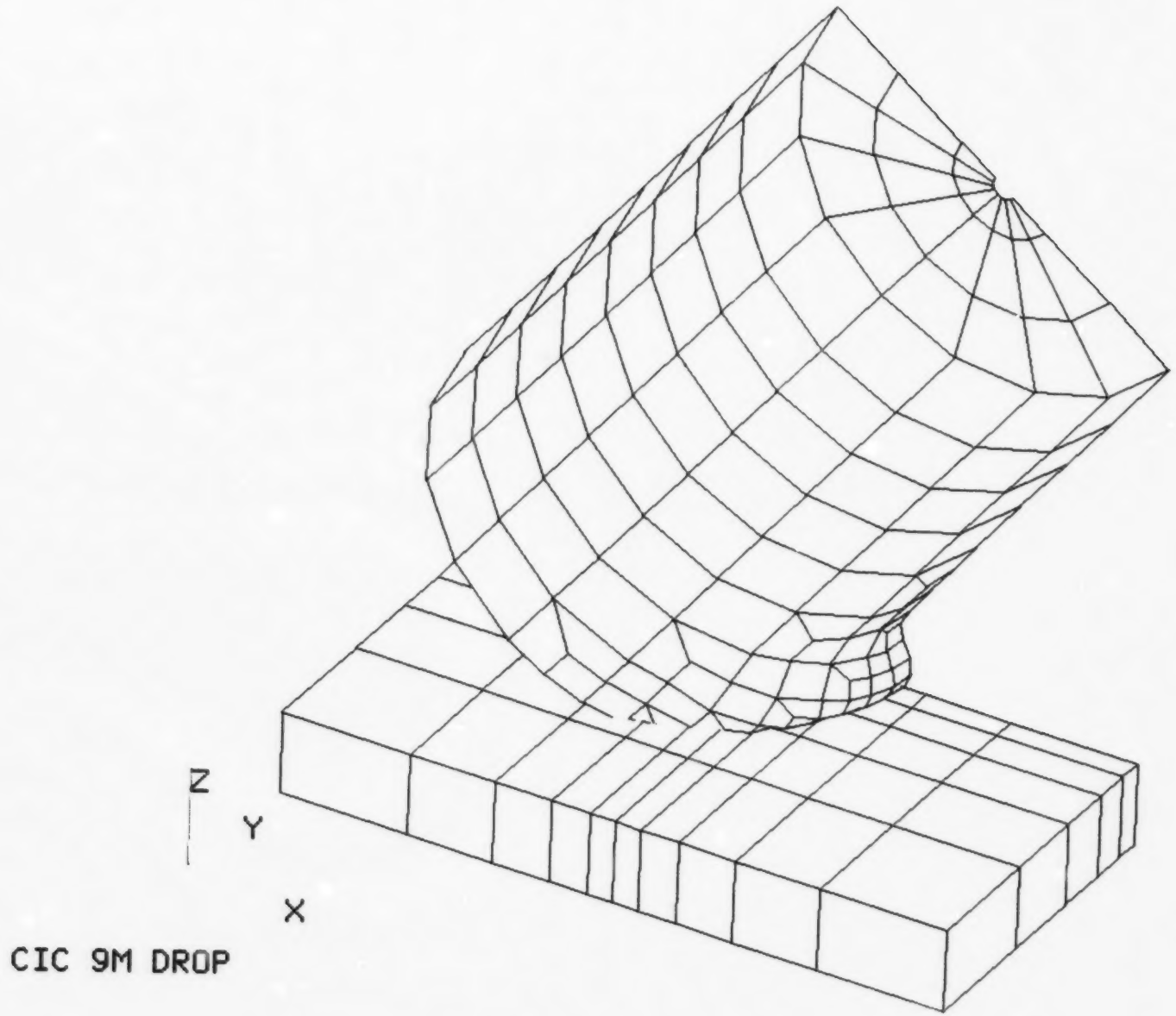


FIG. 21 FINAL DEFORMATION OF CONTAINER



89-286

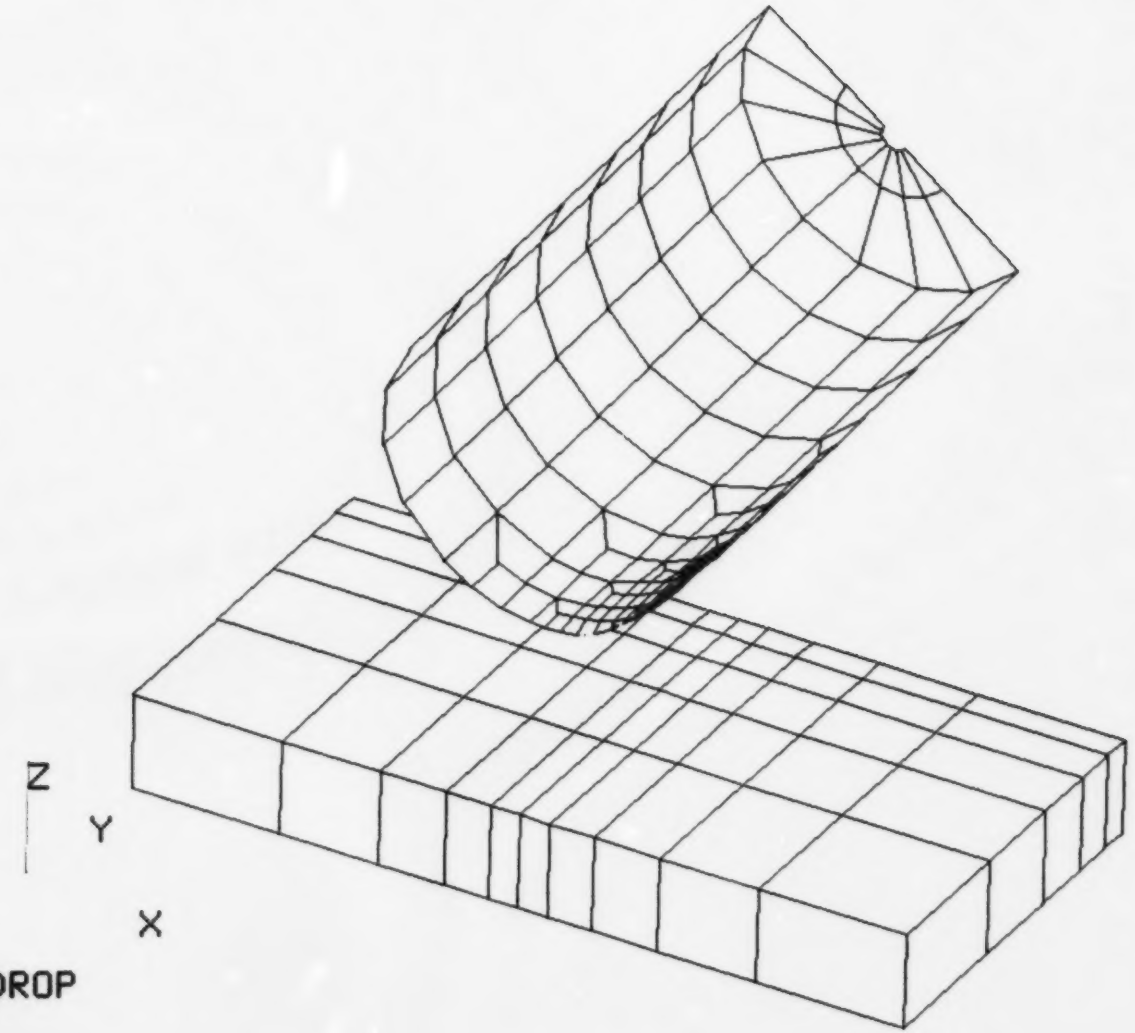


89-286

FIG. 22 FINAL DEFORMATION OF INNER LINER

FIG. 23 FINAL DEFORMATION OF OUTER LINER

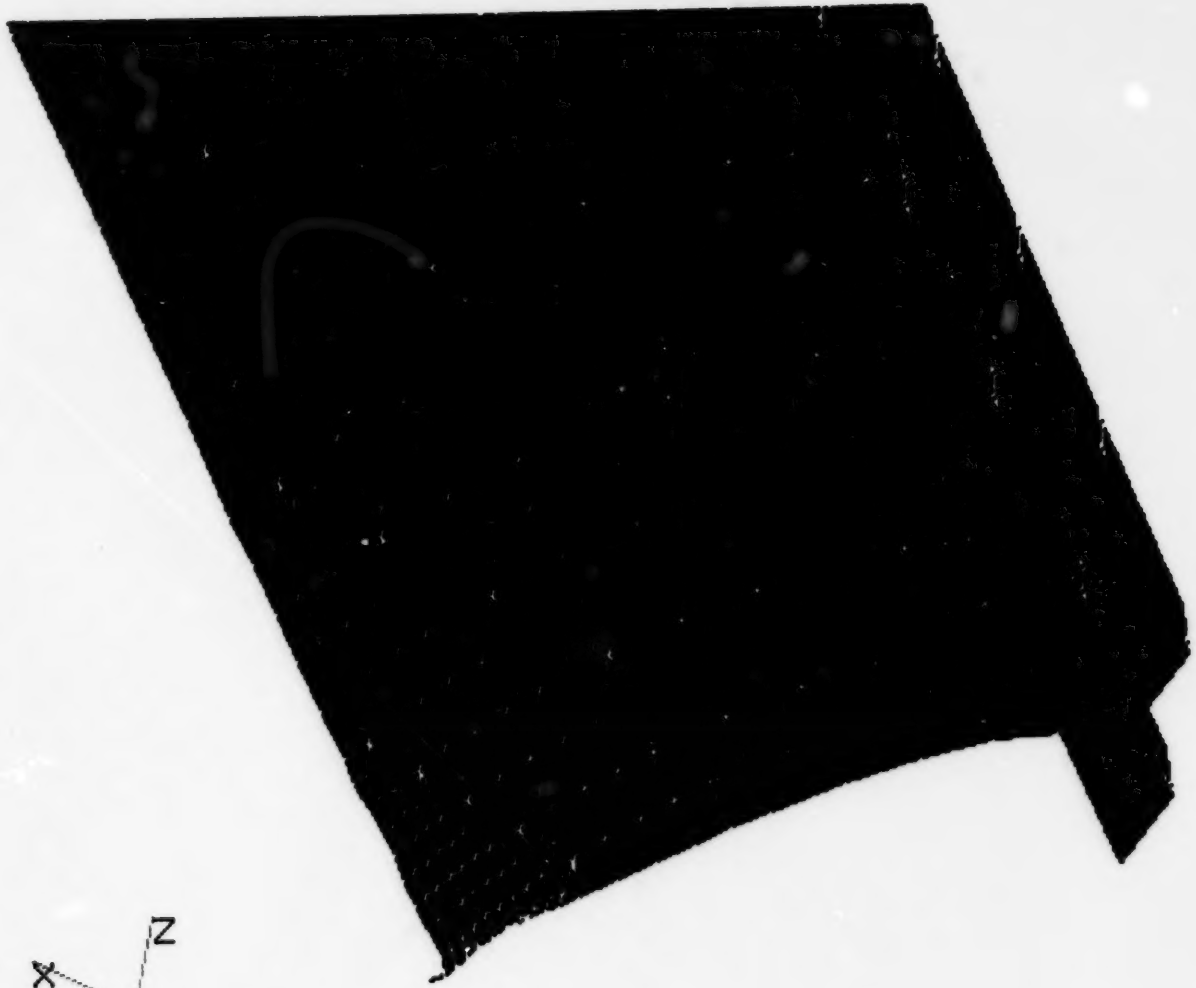


FIG. 24 FINAL DEFORMATION OF INNER LINER

FIG. 25 VON MISES STRESS AT INNER SURFACE OF OUTER LINER (Pa)

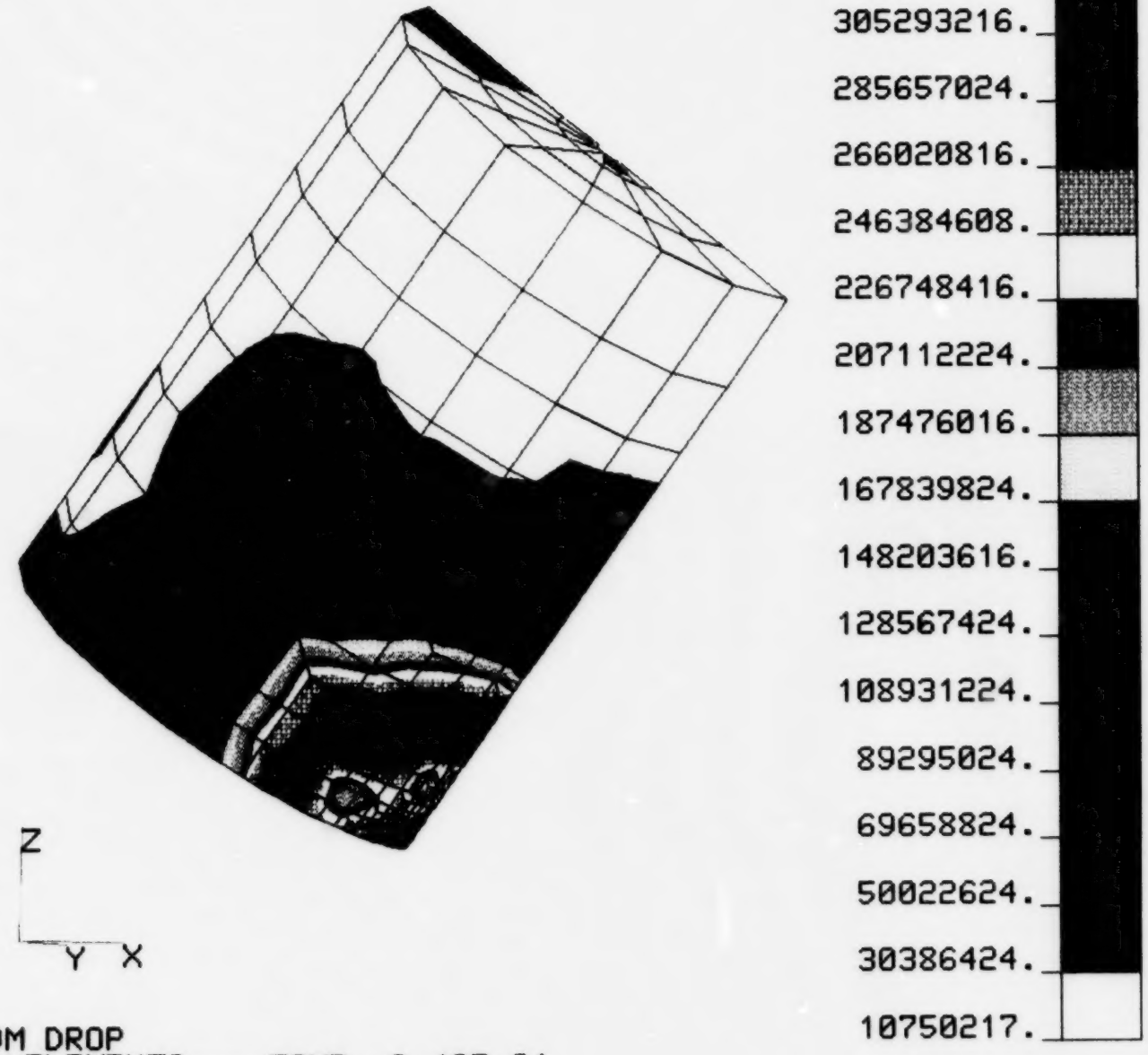


FIG. 26 VON MISES STRESS AT MIDDLE SURFACE OF OUTER LINER (Pa)

FIG. 27 VON MISES STRESS AT OUTER SURFACE OF OUTER LINER (Pa)

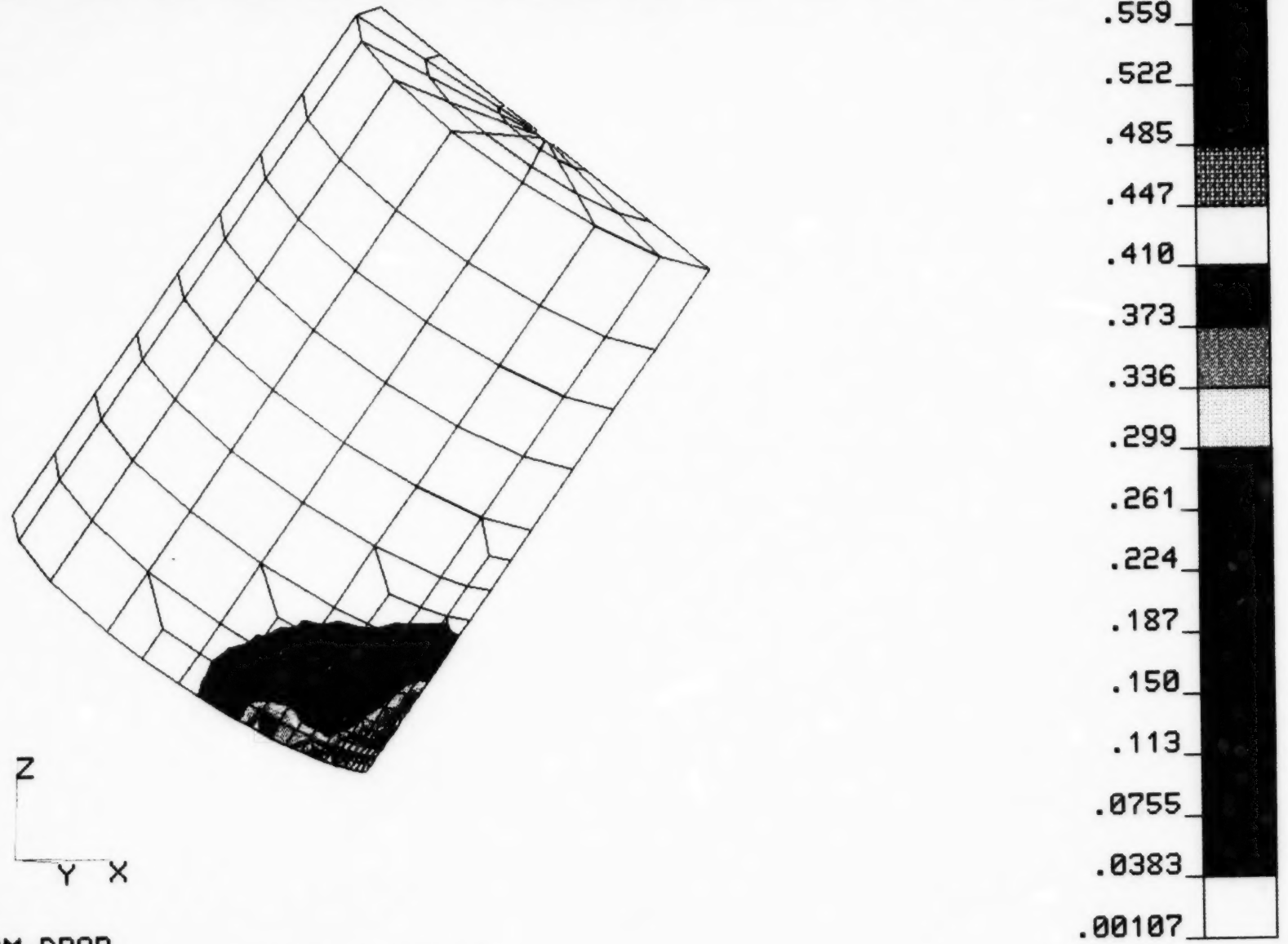


FIG. 28 EQUIVALENT PLASTIC STRAIN AT INNER SURFACE OF OUTER LINER

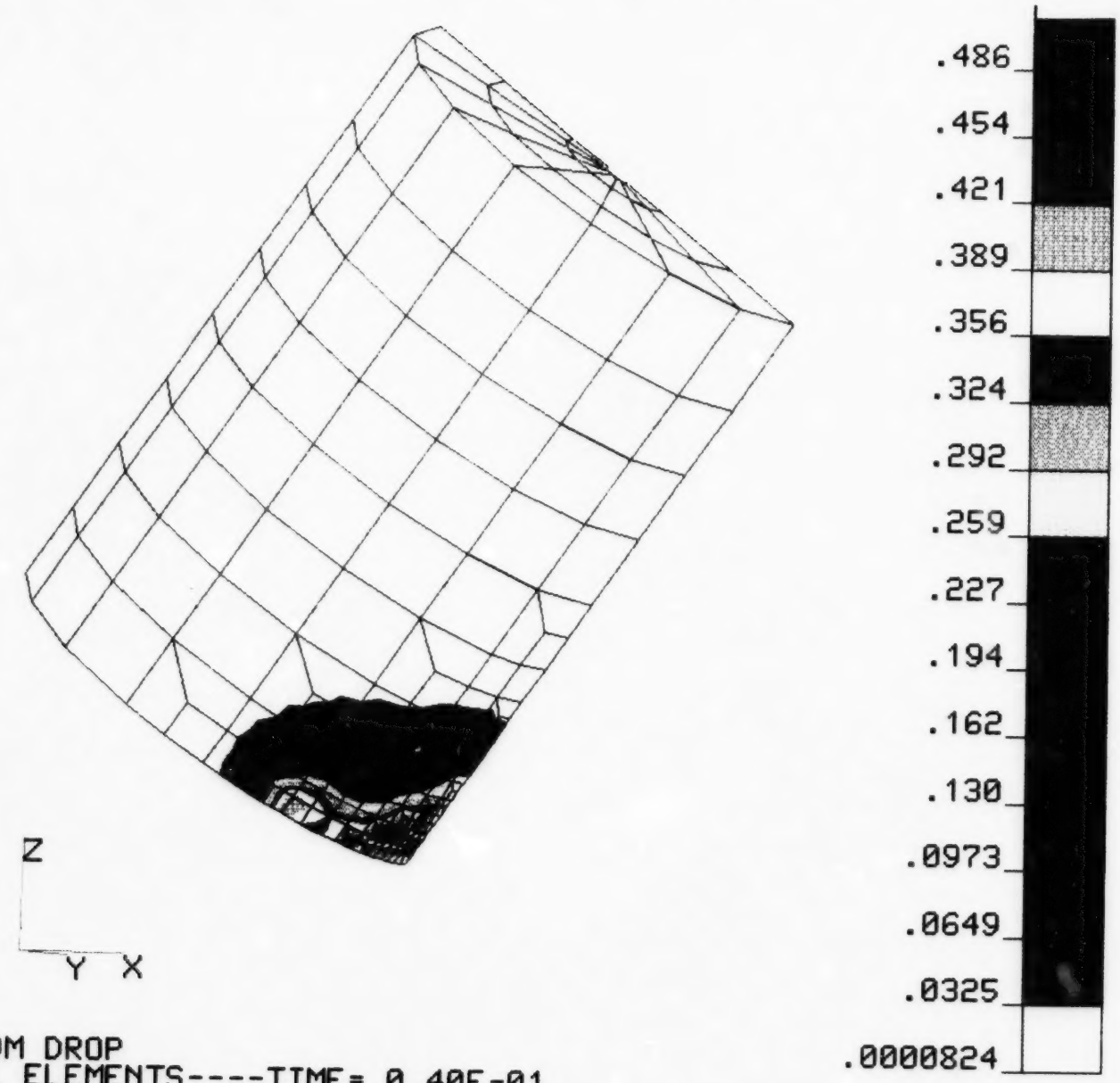


FIG. 29 EQUIVALENT PLASTIC STRAIN AT MIDDLE SURFACE OF OUTER LINER

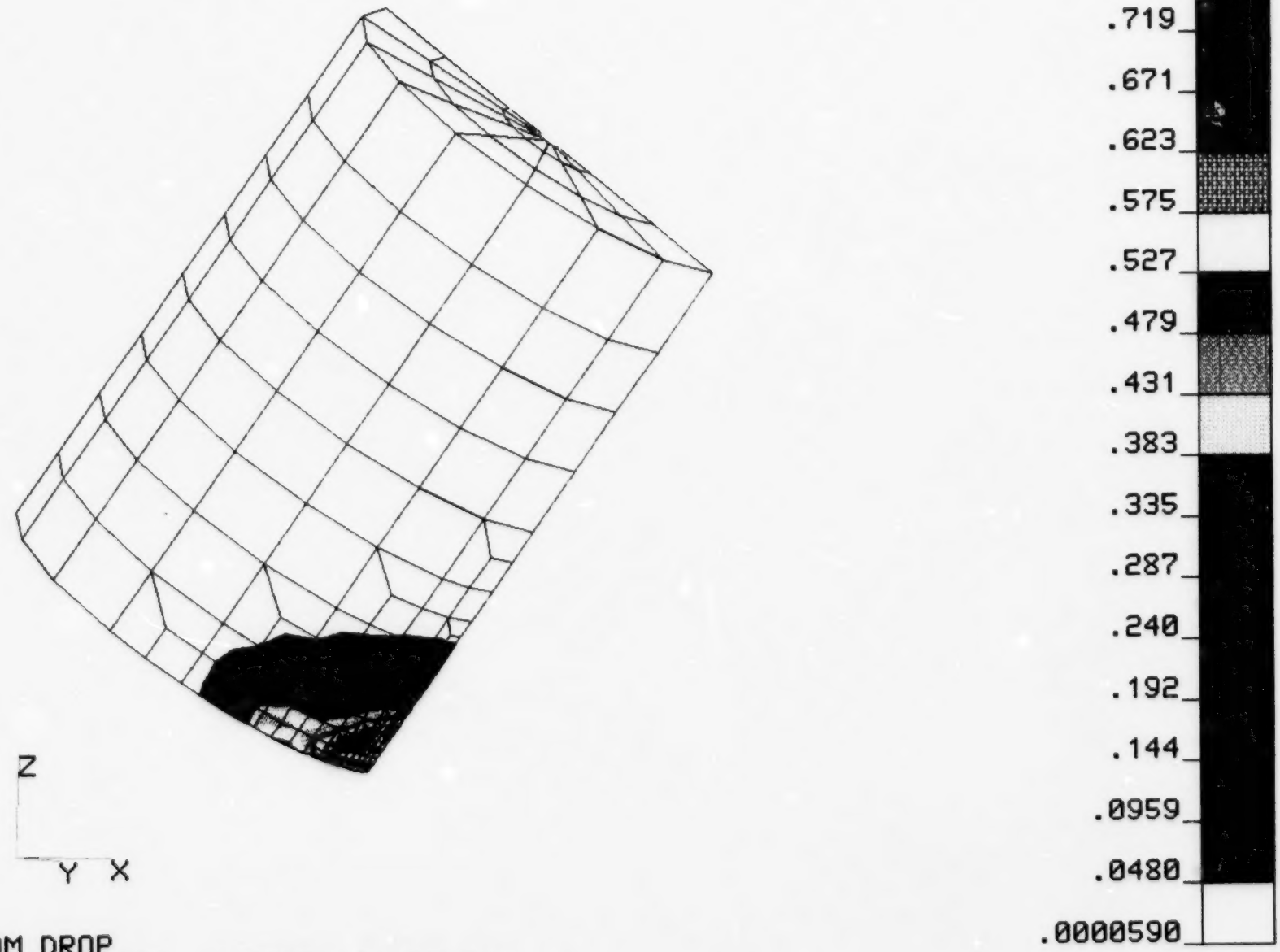




FIG. 30 EQUIVALENT PLASTIC STRAIN AT OUTER SURFACE OF OUTER LINER

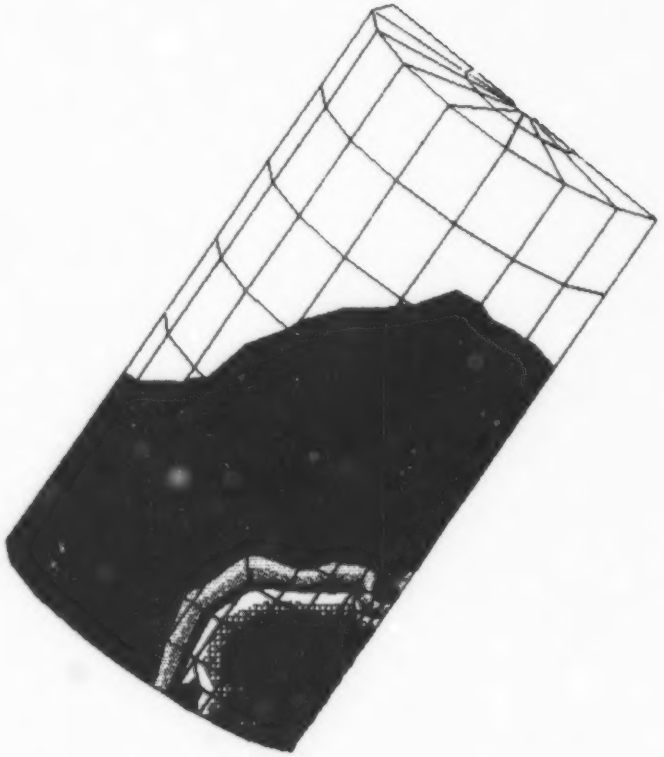

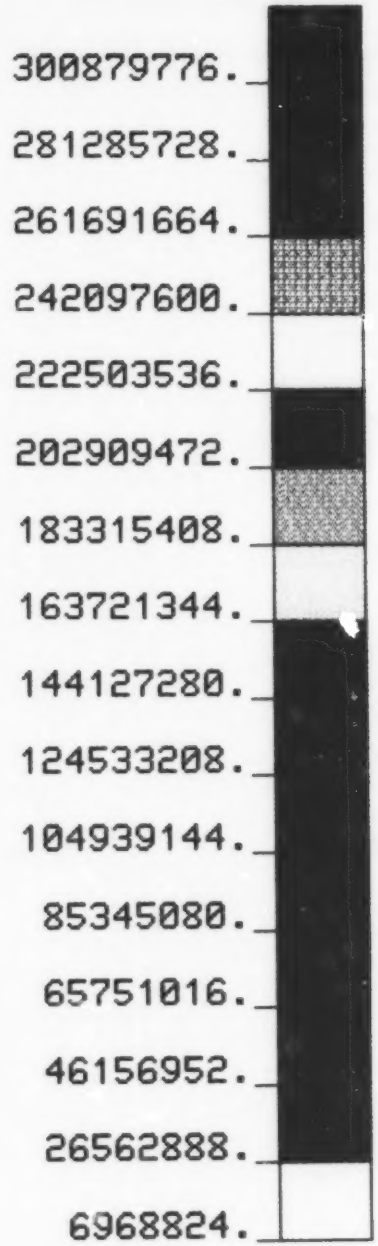

89-286

CIC 9M DROP
SHELL ELEMENTS----TIME= 0.40E-01

FIG. 31 VON MISES STRESS AT MIDDLE SURFACE OF INNER LINER (Pa)

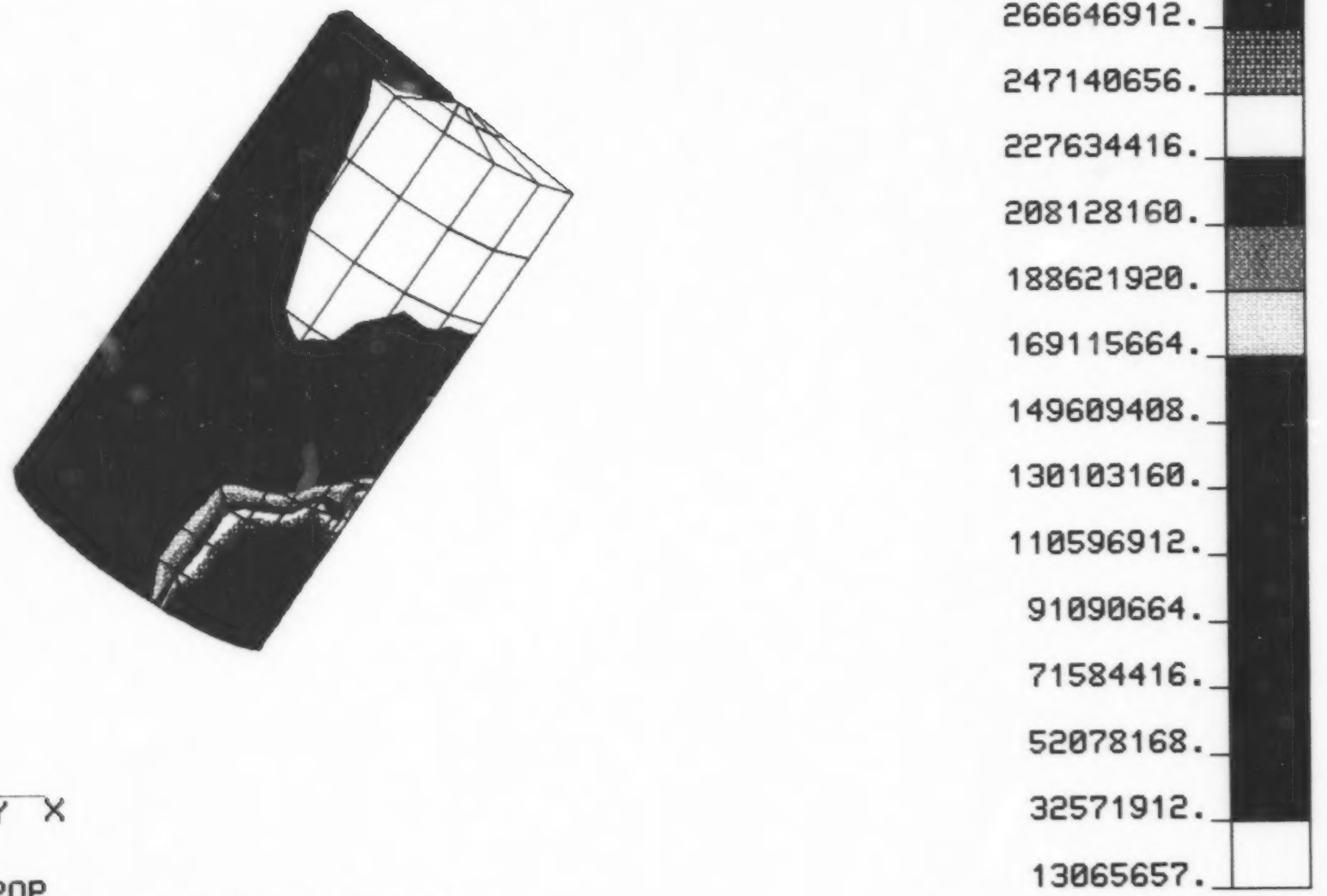




89-286

FIG. 32 VON MISES STRESS AT OUTER SURFACE OF INNER LINER (Pa)

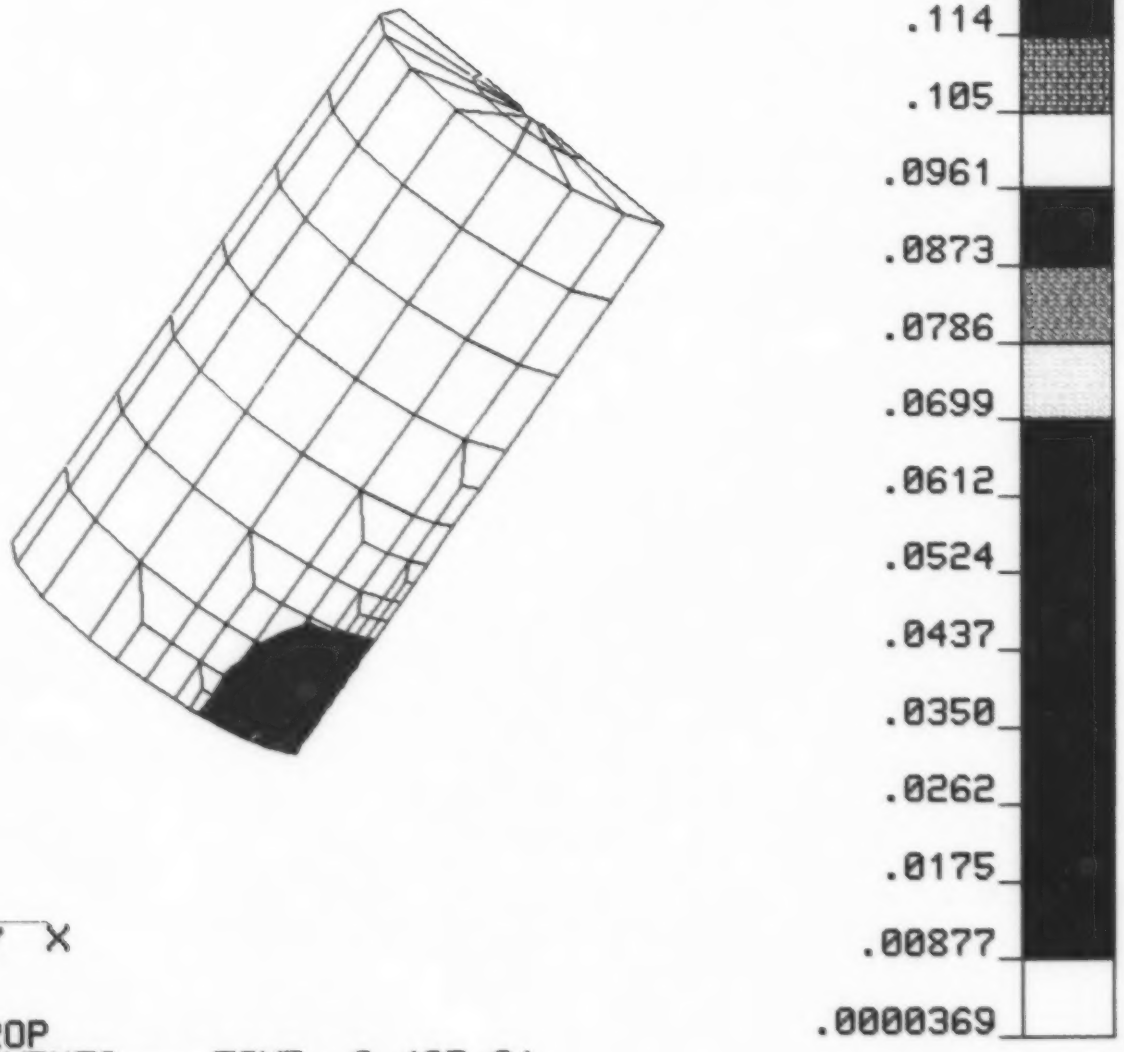


FIG. 33 EQUIVALENT PLASTIC STRAIN AT MIDDLE SURFACE OF INNER LINER

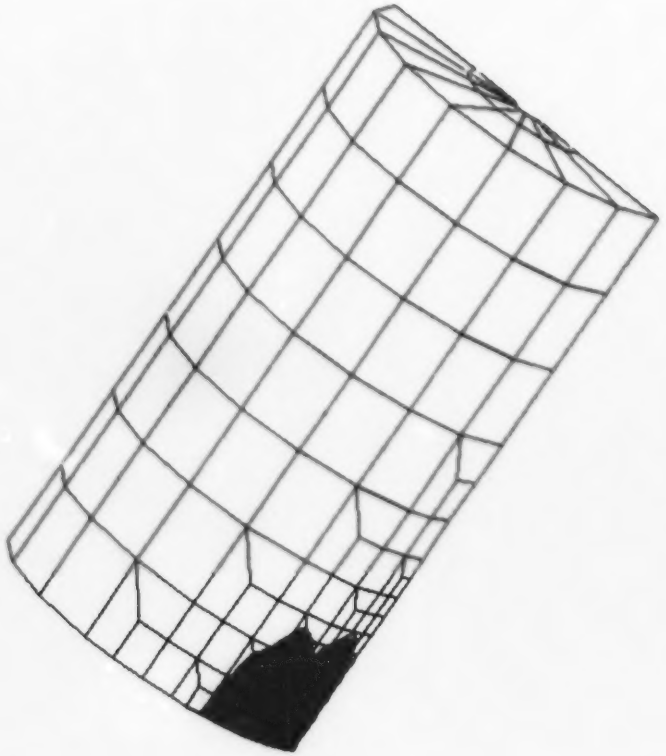


.285
.266
.247
.228
.209
.190
.171
.152
.133
.114
.0950
.0760
.0570
.0380
.0191
.0000561

CIC 9M DROP
SHELL ELEMENTS----TIME= 0.40E-01

FIG. 34 EQUIVALENT PLASTIC STRAIN AT OUTER SURFACE OF INNER LINER

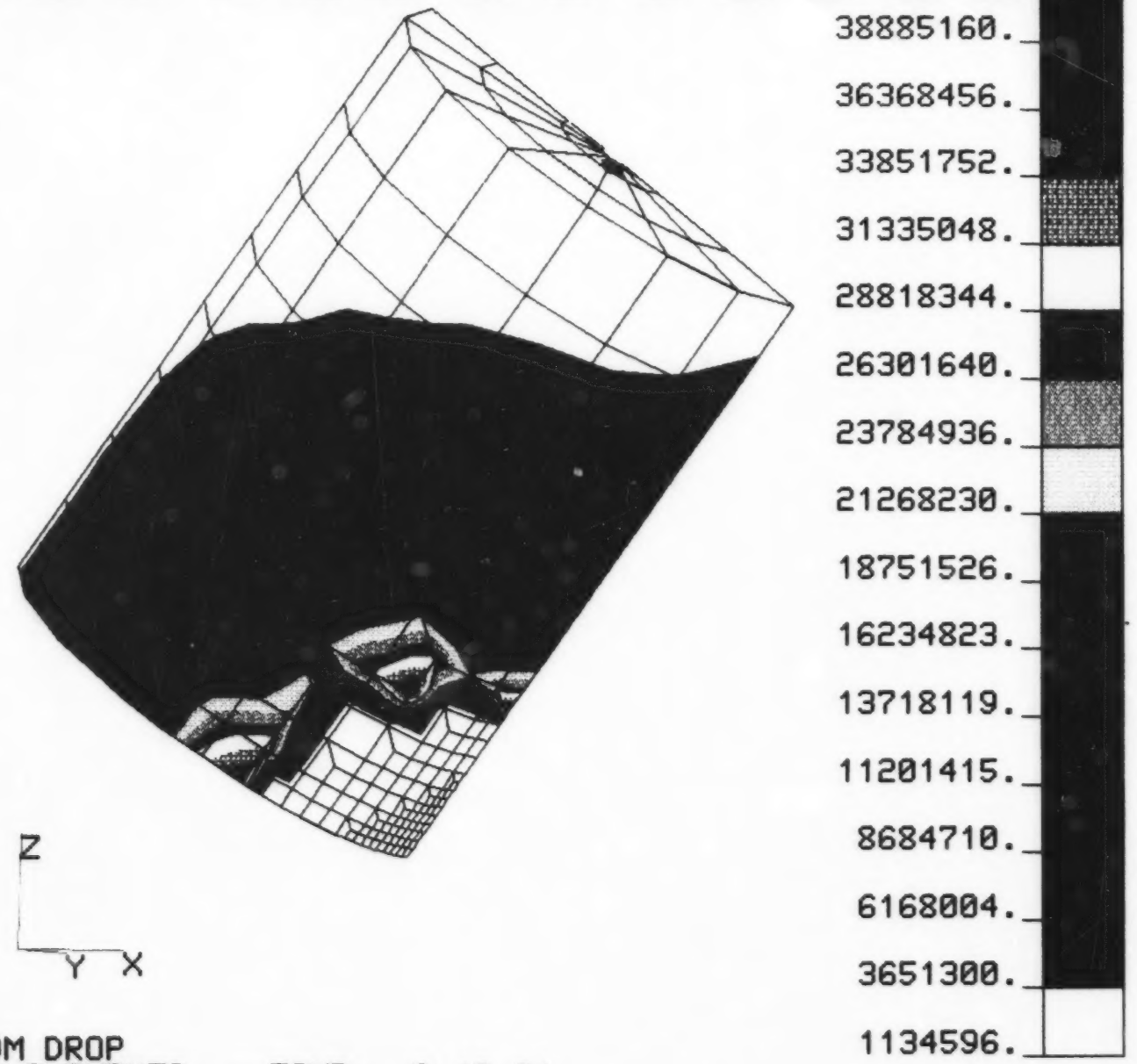


FIG. 35 VON MISES STRESS IN CONCRETE (Pa)

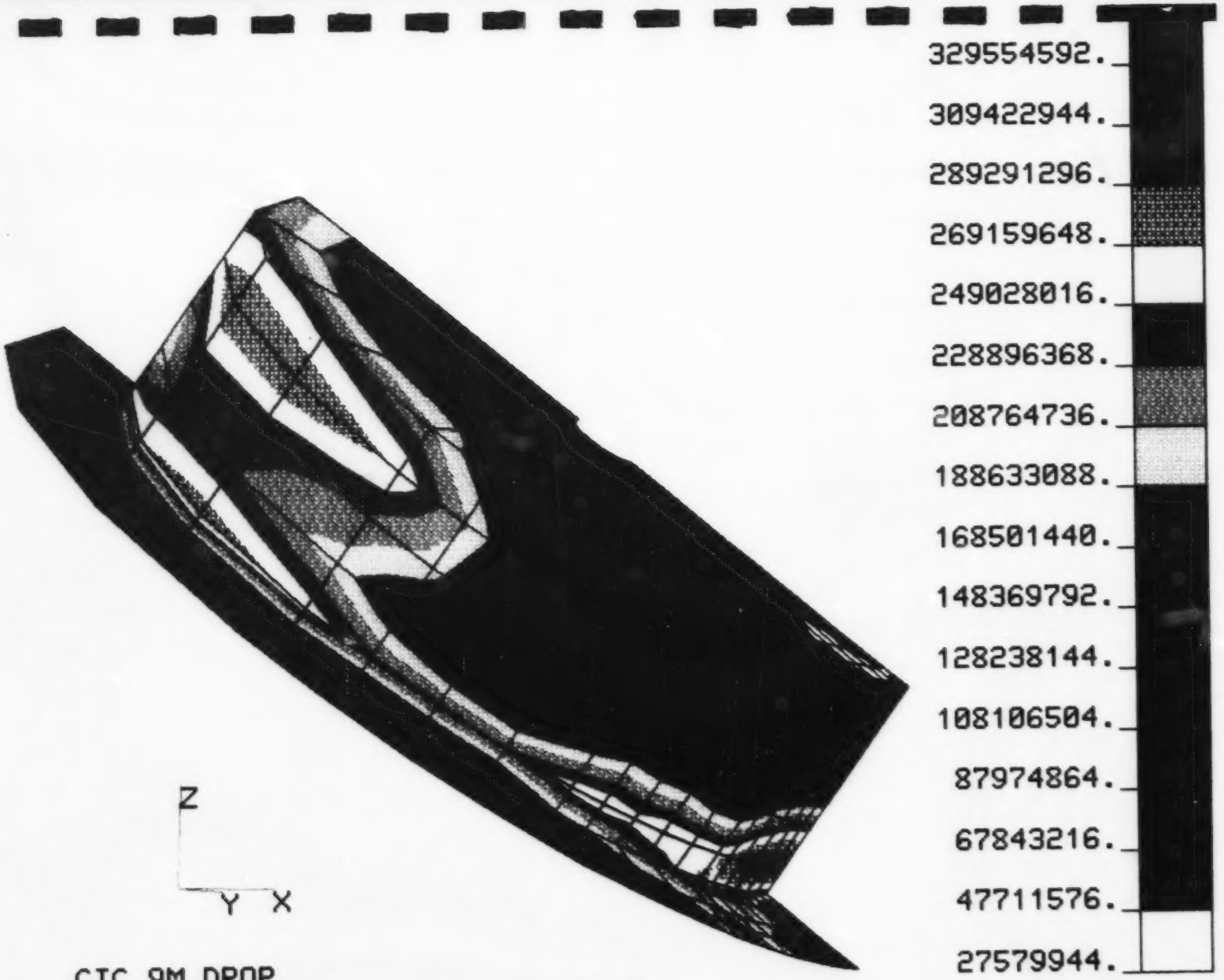


FIG. 36 VON MISES STRESS IN LID STEEL PLATE (Pa)

# APPENDIX A

## SOME FUNDAMENTAL UNDERSTANDINGS OF AN IMPACT PROBLEM

## APPENDIX A

## TABLE OF CONTENTS


| | | Page |
|---|---|---|
| 1.0 | INTRODUCTION | A-1 |
| | 1.1 Global Effect | A-1 |
| | 1.2 Local Effect | A-1 |
| 2.0 | DESCRIPTION OF THE MOTION OF A CONTINUUM | A-2 |
| 3.0 | FIELD EQUATIONS OF A CONTINUUM | A-4 |
| | 3.1 Conservation of Mass | A-4 |
| | 3.2 Conservation of Momentum | A-4 |
| | 3.3 Conservation of Energy | A-5 |
| 4.0 | MATERIAL PROPERTIES (CONSTITUTIVE EQUATIONS) | A-6 |
| | 4.1 Equation of State | A-7 |
| | 4.2 Stress-Strain Relation | A-7 |
| | 4.2.1 Elasticity | A-7 |
| | 4.2.2 Plasticity (Material Non-Linearity) | A-8 |
| | 4.2.2.1 Yield Criterion | A-9 |
| | 4.2.2.2 Hardening | A-10 |
| | 4.2.2.3 Flow Rule | A-12 |
| | 4.2.3 Viscous Fluid | A-12 |
| 5.0 | SHOCK WAVES | A-13 |
| 6.0 | APPLICATION OF CONTINUUM MECHANICS IN IMPACT PROBLEM | A-15 |
| | 6.1 Lagrange Computation | A-15 |
| | 6.2 Euler Computation | A-16 |
| | FIGURES | |

# APPENDIX A

## SOME FUNDAMENTAL UNDERSTANDINGS OF AN IMPACT PROBLEM

### 1.0 INTRODUCTION

The impact problem involves a projectile with a finite amount of mass and velocity impacting onto a target. The impact load should be firstly clarified from another type of the so called impulse load (e.g., jet impingement, compartment pressurization). Even though both are localized transient type of loading, the impact load is different from impulse load by its representation of a finite amount of kinetic energy transferring from a colliding projectile to a target. If the target is a stationary unyielding surface, the projectile will transfer the kinetic energy into strain energy within itself through deformation. The characteristics and the magnitude of the impact are dependent upon and hence determined by the inertial, geometrical and material properties of the projectile as well as the target. It generates higher stresses at a smaller contact area than that of impulse load. Furthermore, the impact load would cause both the global as well as the local effects on the structure, whereas, the impulse load causes mostly the global effect only. These two types of effect are briefly discussed in the following.

### 1.1 Global Effect

Similar to a structure under any type of dynamic or static load, the structure will deform and react when subjected to an impact. This is considered as overall response of the structure and is categorized as the global effect. In this case, the impact load is usually characterized as a force time history and the overall response considering flexure and reaction in the structure can be theoretically analyzed using the conventional dynamic analytical techniques. This means that a set of equations of motion for a multi-degree of freedom system are solved in time or frequency domain using well established numerical solution procedures, either finite element or finite difference formulation. Quite often the analysis can be conservatively simplified to a single degree of freedom system and the analysis most likely would be a non-linear one where an elasto-plastic system is treated. The analytical result in terms of bending moment, shear force and ductility ratio are then investigated and evaluated as the available resisting strength of the structure against impact load.

### 1.2 Local Effect

For an impact problem, in addition to the global effect, structure will be subjected to local damages such as penetration, perforation, spalling and scabbing. These are categorized as local effects which occur in a very short duration of time prior to the full development of global effect. In this case it is assumed that only a region of structural element in the vicinity of the impact location participates in energy absorption. Hence, unlike the global effect the local effects are largely independent of the dynamic characteristics of the overall structure.

Analytical prediction of local effect is much more difficult than that of global effect due to the complex nature of the transient stress state. At the area of contact extreme high bulk stress may be generated due to sudden decelerations of projectile and hence crush the project and/or target material. Two types of waves, the longitudinal and the translational waves, will be generated and radiated out from impact point. The longitudinal wave which initially travels at the sound speed of the material causes material volume change and the translational wave which travels at a lower speed distorts the material body. After reaching the back face of the structural element, the waves reflect and travel in the opposite direction. The reflected longitudinal wave reverse the stresses from compression to tension which, when reached the tensile strength limit of the material, will cause cracking and result in back face scabbing. When this tension wave travels further toward the original impacting location where the material has been crushed and left no tensile strength, a front face spalling might occur. On the other hand, if the distortional energy generated in the material exceeds its limit, the material will yield and response plastically. The crushing and yielding of the material make the prediction of local effect a geometrical and material non-linear analysis and the spalling and scabbing cause the material large deformation with significant amount of mass flow. Consequently, the conventional dynamic analysis method as mentioned earlier in the global effect is no longer adequate to describe the motion of the system. Some more fundamental principles of continuum mechanics based on the conservation of the mass, momentum and energy within the system has to be applied. In short, to evaluate local effect using continuum formulation will take the wave propagation into account; whereas, the evaluation of global effect using conventional structural formulation will not. It is this local effect which has been the major concern for the present investigation.

## 2.0 DESCRIPTION OF THE MOTION OF A CONTINUUM

A continuum can be either a solid or a fluid which moves when subjected to an external agency. The motion of a continuum should follow certain rules so that the boundary conditions and the physical characteristics of the continuum will not be violated. Material-wise, most continuum obey Newton's Law of Motion. The rules to be followed are the laws of conservation of mass, momentum and energy. Due to its complexity, the problem has to be solved using a numerical approach. Methodologically, the material body is discretized to a set of mesh system (finite elements) or grid system (finite difference). Each small piece of material body bounded by the grid lines forms the basic spatial domain to be dealt with using continuum mechanics.

Based on different reference coordinate systems there are two ways to describe the motion of a continuum, namely, the Lagrange frame (material description) and the Euler frame (spatial description).

In Lagrange, the transformation of a spatial domain to another is based on the coordinate of a continuum on a particle by particle basis. This means that the motion of each particle in the continuum is historically updated and recorded. Hence, the velocity and the acceleration of individual particle are described. The Lagrange can be conveniently used for describing a solid which usually experience smaller deformation and the coordinate of individual

particle can be traced without difficulty. This is done by evaluating the mass, momentum and energy of a zone (the basic spatial domain) and subsequently distributing them to the grid points (nodes). At each grid point the contributed mass, momentum and energy from the surrounding zones are summed. The force and the deformation in terms of acceleration, velocity and displacement are then evaluated at the grid point.

On the other hand, in Euler, a fixed global coordinate is provided and the position of individual particle is not traced. Within a given spatial domain the instantaneous motion of the continuum is described by a velocity field which is the velocity of a particle instantaneously located in that domain and the acceleration of the particle is then derived from that velocity field. The Euler is most suitable for a continuum involving very large deformation such as flow of a fluid and it has been traditionally used in hydrodynamics. In this case the basic spatial domain can be viewed as a cell where material flow through. The grid lines which bound the cell form the boundary surface for the spatial domain. The mass, momentum and energy are evaluated over the fixed domain and the deformation in terms of velocity is usually evaluated at the center of the cell. The force in this case is not directly dealt with, Instead, the impulse has been used in the consideration of balance of momentum.

In continuum mechanics a strain rate - velocity relationship are used to replace the conventional strain-displacement relation for describing material flow. Actually the analysis of the velocity field is very much like the analysis of an infinitesimal deformation field in a solid. Quite often it is the material integrals which represent the total amount of certain quantity associated with a given continuum body are dealt with (e.g., the mass, momentum and energy over certain volume of a continuum). In such a case the integral becomes only the function of time and the material derivative of a volume integral (i.e., the rate of change of a material integral) can be written as:

$$\frac{D}{Dt}\left(\int_v A\,dv\right) = \frac{d}{dt}\left(\int_v A\,dv\right) + \oint_s A\vec{V}\cdot d\vec{S} \qquad (1)$$

Details of derivation of this equation can be found in any textbook of continuum mechanics even though it may be expressed in different form. In the equation, A represents a unit quantity such as density, unit momentum, and specific energy etc. The first term on the right hand side is the rate of the change of material integral over the volume at beginning of an instantaneous time; the second term represents the material transport through the body surface where $\vec{V}$ and $\vec{S}$ are the velocity and surface area vectors respectively. If the Lagrange coordinate system is used, the second term in the equation vanishes. This is the most important equation which is the mathematical expression of conservation of mass, momentum and energy when such quantities are substituted into the equation. A set of governing field equations can then be derived and solved with given material properties. They are summarized in the following:

## 3.0 FIELD EQUATIONS OF A CONTINUUM

### 3.1 Conservation of Mass

The mass contained in a spatial domain is:

$$m = \int_v \rho \, dv \tag{2}$$

Where $\rho = \rho(x,t)$ is the density of the continuum at the location x and time t. Conservation of mass requires that $Dm/Dt = 0$. Applying Equation 1 and replacing A by $\rho$ results the so called equation of continuity in the Euler coordinate system as:

$$\frac{dm}{dt} + \oint_s \rho \vec{V} \cdot d\vec{s} = 0 \tag{3}$$

In the Lagrange coordinate system the second term vanishes which leads to $dm/dt = 0$. Hence the conservation of mass is automatically satisfied.

### 3.2 Conservation of Momentum

Newton's law of motion states that in an inertial frame of reference the material rate of change of the linear momentum of a continuum is equal to the resultant of applied forces. The linear momentum M in the spatial domain v at the time t is:

$$M_i = \int_v \rho V_i \, dv \tag{4}$$

where V is velocity and subscript i (and j and k which appear later) is the conventional tensor notation for x, y and z.

Applying Equation 1 and substituting $\rho V_i$ for A, the Euler's equation of motion based on Newton's law is as follows:

$$\frac{DM_i}{Dt} = \frac{dM_i}{dt} + \oint_s \rho V_i \vec{V} \cdot d\vec{s} = F_i \tag{5}$$

where the resultant force $F_i$ over the continuum body is

$$F_i = \oint_s \sigma_{ij} \, ds$$

OR $$- \int_v \frac{\partial \sigma_{ij}}{\partial X_j} \, dv \qquad (6)$$

The transformation of a surface integral into a volume integral in Equation 6 can be performed using Gauss' theorem.

In the Lagrange coordinate system the second term in Equation 5 vanishes. Substituting Equation 4 and 6 into 5 and performing some mathematical manipulation with the aid of conservation of mass, the equation of motion can be written as follows:

$$\rho a_i = \frac{\partial \sigma_{ij}}{\partial X_j} \qquad (7)$$

where $a_i = \partial V_i / \partial t$ are acceleration components.

3.3 Conservation of Energy

The law of conservation of energy is the first law of thermodynamics. If thermal process is significant, the equation of energy including heat is an independent equation to be satisfied. If mechanical energy alone is of interest such as in the present study, the energy equation is merely the first integral of the equation of motion.

There are three forms of energy in a continuum, the kinetic energy KE, the gravitational (potential) energy GE, and the internal energy IE. They are expressed as follows:

$$KE = \int_v \frac{1}{2} \rho V_i \; V_i \, dv \qquad (8)$$

$$GE = \int_v \rho \, \Phi \, dv \qquad (9)$$

$$GE = \int_v \rho \, e \, dv \qquad (10)$$

where $\Phi$ is the gravitational potential per unit mass and e is the specific internal energy (internal energy per unit mass).

The conservation of energy states that the rate of change of energy of a continuum is equal to the rate of work done on the system and is expressed as:

$$\frac{D}{Dt}\,(KE + GE + IE) = \dot{W} \tag{11}$$

where the rate of work on a continuum is:

$$\dot{W} = \oint_s \sigma_{ij} v_i ds_j$$

OR

$$= \int_v (\sigma_{ij} v_i)_{,j} dv \tag{12}$$

Substituting Equation 8, 9, 10 and 12 into Equation 11 and applying Equation 1; and after lengthy manipulations with application of equation of continuity, equation of motion and strain rate-velocity relation, the equation of energy can be written in Euler frame as:

$$\frac{d(IE)}{dt} + \oint_s \rho e \vec{V} \cdot \vec{ds} = \int_v \sigma_{ij} \dot{\epsilon}_{ij}\, dv \tag{13}$$

Equation 13 can be written in a differential form as;

$$\rho \left( \dot{e} + V_j \frac{\partial e}{\partial x_j} \right) = \sigma_{ij} \dot{\epsilon}_{ij} \tag{14}$$

In the Lagrange coordinate system, the convective term (the second term) vanishes and the equation simply becomes

$$\rho \dot{e} = \sigma_{ij} \dot{\epsilon}_{ij} \tag{15}$$

## 4.0 MATERIAL PROPERTIES (CONSTITUTIVE EQUATIONS)

An equation which describes the properties of a material is called a constitutive equation of that material. Two types of constitutive equations are involved in the present study:

(a) An equation to describe pressure-volume relationship (equation of state);

(b) An equation to describe stress-strain relationship.

## 4.1 Equation of State

The equation of state relates pressure to volume change and specific internal energy of the material. Since the volume is relevant to the change of density, the equation can be expressed as a function of density and specific internal energy as:

$$P = f(\rho, e) \tag{16}$$

Equation 16 is usually obtained from experiments on material.

In the conventional structural analysis, the equation of state is not required because the material is considered "solid"; hence, the volume change and the body pressure would not affect each other significantly. This is not necessary so in a continuum where material is considered a fluid with motion such as a typical hydrodynamic problem.

Other equations of state, such as the one to describe heat transfer characteristics, is not considered because thermal effect on the material is ignored in this study.

## 4.2 Stress-Strain Relation

### 4.2.1 Elasticity

For a solid material in elastic range, the constitutive equation is simply the Hook's law:

$$\sigma_{ij} = C_{ijkl}\, \epsilon_{kl} \tag{17}$$

where $C_{ijkl}$ is the tensor of elastic constant.

When the material is istropic $C_{ijkl}$ are reduced to two constant terms, $\lambda$ and G (Lame's Constants), and Equation 17 is simplified to:

$$\sigma_{ij} = \lambda \epsilon_{kk} \delta_{ij} + 2\, G \epsilon_{ij} \tag{18}$$

where $\delta_{ij}$ is the Kronecker delta and the strain can be separated into deviatoric and mean strain parts.

$$\epsilon_{ij} = \epsilon'_{ij} + \frac{2}{3}\, \epsilon_{kk}\, \delta_{ij} \tag{19}$$

Substituting Equation 19 into 18 results in:

$$\sigma_{ij} = K\epsilon_{kk}\delta_{ij} + 2G\epsilon'_{ij}$$

OR

$$= \frac{1}{3}\sigma_{kk}\delta_{ij} + 2G\epsilon'_{ij}$$

OR

$$= -P\delta_{ij} + 2G\epsilon'_{ij} \qquad (20)$$

where $K=(3\lambda + 2G)/3$ is the bulk modulus (coefficient of volume expansion) of the material; G is the shear modulus; and $p = -\sigma_{kk}/3$ is the mean normal stress and is referred as hydrostatic pressure. The second term on the right hand side of Equation 20 represents the stress deviation.

$$\sigma'_{ij} = 2G\epsilon'_{ij}$$

$$= 2G(\epsilon_{ij} - \frac{1}{3}\epsilon_{kk}\delta_{ij}) \qquad (21)$$

Expressing in term of rate form, Equation 21 becomes:

$$\dot{\sigma}_{ij} = 2G(\dot{\epsilon}_{ij} - \frac{1}{3}\dot{\epsilon}_{kk}\delta_{ij}) \qquad (22)$$

### 4.2.2 Plasticity (Material Non-Linearity)

When a material yields, the constitutive equation has to be derived with application of the theory of plasticity. There are two major plasticity theories: the total (deformation) theory and the incremental (flow) theory. The deformation theory assumes that a unique relation between total stresses and total strains exists. The total strain components are functions of current state of stresses and are independent of the loading path. This is in contradiction with the experimentally determined properties of material and hence its use is limited. On the other hand, in the flow theory, only incremental stresses and strains are related. The incremental plastic strain components at any instant of loading are assumed to be proportional to the corresponding instantaneous deviatoric stresses. Plastic deformations are traced by integrating the plastic strain increments over the previous loading history. The incremental theory is widely accepted and is suitable for the analysis of impact problem where the numerical integration of the governing differential equations are proceeded incrementally (step by step) in time domain.

The plastic behaviour of a material in a multi-axial state can be described by specifying the following three parts which make up the content of the incremental theory.

(a) A yield criterion which defines the elastic limit of the material in a multi-stress state

(b) A hardening rule which specifies the changes in shape and orientation of the yield surface for subsequent yield from a plastic state

(c) A flow rule which provides the constitutive relations between incremental plastic strains and current state of stresses

4.2.2.1 Yield Criterion

A yield condition can generally be described in the form:

$$f(\sigma_{ij}, c) = 0 \tag{23}$$

where c is a parameter representing plastic strain or hardening characteristic. The function f is termed a yield function in the case of initial yielding and is referred to as a subsequent yield function or loading function in the case of subsequent yielding. This function represents a hypersurface to bound all the accessible states which can be achieved in an actual material element by some program of stressing. By temporarily fixing c as a constant at an instantaneous time, the hypersurface can be projected onto the stress space and is called the yield surface. The yield surface, similar to the hypersurface, bounds the elastic region in the stress space for a particular stress-strain history c. Yield surfaces generated by changes in c during a stress program are referred to as the subsequent yield surfaces or loading surfaces.

Equation 23 has often been expressed in an alternate form:

$$f(\sigma_{ij}) = K \tag{24}$$

where k represents some yielding parameter which is a constant for the case of initial yielding and is a function of the previous stress and strain history of the material and its hardening properties for the case of subsequent yielding from a plastic state. If the material is elastic-perfectly plastic (non-hardening), k remains a constant.

One specific form of Equation 24 (Drucker and Prager) is

$$f = \alpha I_1 + J_2^{1/2} = K \tag{25}$$

where $\alpha$ is a positive constant; $I_1 = \sigma_{ii}$ is the first invariant of stress tensor; and $J_2 = \frac{1}{2}\sigma'_{ij}\sigma'_{ij}$ is the second invariant of the stress deviation. Physically the first term represents the volume change (dilatancy) of the material body and the second term the distoration of the body.

Among many proposed yield criteria, the Von Mises criterion is the one most commonly used (particularly for metals). The Von Mises yield criterion assumes that yielding begins when the distortion energy equals the distortion energy at yield in a simple tension test. Since the internal energy due to distortion can be expressed in terms of the octahedral shear stress or the second invariant of the deviatoric stress tensor ($J_2$), two alternate ways of stating the criterion are respectively: (1) Yielding begins when the octahedral shear stress exceeds a limit (i.e., the octahedral shear stress in simple tension). The octahedral plane is referred to the principal stress directions. and (2) Yielding begins when $J_2$ reaches a critical value (i.e., the value of $J_2$ in simple tension).

Of the two forms of expression, the one using $J_2$ is most commonly adopted. Introducing the critical value of $J_2$ in an uniaxial tensile test, which is equal to $Y^2/3$, the Von Mises yield criterion is written as:

$$J_2 = \frac{1}{3} Y^2$$

OR

$$(3J_2)^{1/2} = Y \qquad (26)$$

where Y is the initial yield strength in a uniaxial tensile test.

Comparing Equation 25 and 26, the $I_1$ term in Von Mises criterion is not taken into account. This implies that the pressure (mean stress) which cause volume change plays no role in defining material yielding. When projected onto principal stress space, the Von Mises yield surface (Equation 26) is a right circular cylinder with its axis equally inclined to the coordinate axis; whereas, the yield surface of Equation 25 is a right circular core with its apex in the tension octant.

4.2.2.2 Hardening

Work hardening means that for all such added sets of stresses a positive work is done in the material and the net work performed over cycles of application and removal of stresses is either zero or positive. When the stress state of the material lies on the yield surface (i.e., Equation 25 or Equation 26 is satisfied), the departure from the plastic state due to a further load increment may result in three different loading conditions for strain hardening material:

Loading $$df = \frac{\partial f}{\partial \sigma_{ij}} d\sigma_{ij} > 0$$

Neutral Loading $$df = \frac{\partial f}{\partial \sigma_{ij}} d\sigma_{ij} = 0$$

Unloading $$df = \frac{\partial f}{\partial \sigma_{ij}} d\sigma_{ij} < 0$$

The first case of $df > 0$ means that the stress state is moving out from the yield surface and plastic flow is occurring. The second case of $df = 0$ indicates that the stress state is moving on the yield surface and represents perfectly plastic behaviour. The third case of $df < 0$ means that the stress state is moving into the elastic region from the yield surface and is entirely an elastic behaviour.

For a material of perfectly plastic, the case of $df > 0$ does not exist. Its plastic flow actually occurs at the case of $df = 0$. Elastic unloading of $df < 0$ for a perfect plastic material is the same as for a hardening material.

When loading occurs, a hardening rule is required to describe the manner in which the yield surface is modified as the result of plastic deformation. Since a material is physically unable to maintain a stress state outside its yield surface, this modification is necessary to keep the stress state on the subsequent yield surface and to have material capable of maintaining a higher stress state due to work hardening. Many hardening rules have been proposed such as, the isotropic hardening rule, the kinematic hardening rule, the mechanical sublayer model and the Mroz theory. Discussions and comparisons of these models are available in public literature and will not be described in here.

There are two hypotheses often used to measure the amount of hardening:

(a) Work-hardening Hypothesis

In this hypothesis plastic work is used for measurement so that the Y of Equation 26 is a function of the plastic work done on the material which is defined by:

$$\overline{W}^P = \int \sigma_{ij} \, d\epsilon^P_{ij} \tag{28}$$

(b) Strain-hardening Hypothesis

In this hypothesis the equivalent plastic strain is used for measurement so that Y is a function of the recorded plastic strain which is defined by:

$$\epsilon^P_e = \int d\epsilon^P_e \tag{29}$$

Equation 28 and 29 can be obtained from experimental tests such as the stress-strain relationship obtained from uniaxial tensile test for Von Mises yield criterion.

4.2.2.3 Flow Rule

Drucker's Postulate of stability in material leads to the following consequences:

1. The initial yield surface and all subsequent loading surfaces must be convex (convexity).

2. The plastic strain increment vector $d\epsilon^{P}_{ij}$ must be normal to the yield or loading surface (normality).

3. The change of plastic strain is a linear function of the change of stress (linearity).

The normality condition is expressed as:

$$d\epsilon^{P}_{ij} = \lambda \frac{\partial f}{\partial \sigma_{ij}} \tag{30}$$

where $\lambda$ is the non-negative constant of proportionality which varies throughout the loading history. The loading function, f, plays the same role as a plastic potential (theory of plastic potential by Von Mises).

In Equation 30 the linearity can be established by showing $\lambda$ to be independent of all component of $d\sigma_{ij}$ except the component in the direction of the normal $\partial f/\partial \sigma_{ij}$. Once the yielding function is given and substituted into Equation 30, a rule of plastic flow relating plastic strain increment to state of stress can be set up. If the Von Mises yield function of Equation 26 is substituted into Equation 30, the well known associated flow rule of Prandtle - Reuss equation can be obtained. If the $J_2$ in Equation 26 is retained but the Y is evaluated through other yield criterion, then the resulting equation becomes an unassociated flow rule.

After plastic strain increment is known, the total strain increment which is the sum of elastic and plastic components can be readily obtained. An incremental stress-strain relation can then be worked out through mathematical manipulation. Note that the above discussions have been expressed in incremental (space rate) form, similar expressions in the form of time rate can be done which result in a stress rate-strain rate relationship.

4.2.3 Viscous Fluid

Most fluid can be treated as Newtonian type viscous fluid for which the shear stress is proportional to the rate of deformation. The stress-strain relationship is specified by the equation.

$$\sigma_{ij} = -P\delta_{ij} + D_{ijkl}\dot{\epsilon}_{kl} \tag{31}$$

where P is the static-fluid pressure which is related to the density through the equation of state and $D_{ijkl}$ is the tensor of viscosity coefficients of the fluid.

Comparing Equation 17 and Equation 31, it can be seen that the fundamental difference between elasticity and fluid mechanics is the presence of the static fluid pressure in the later case. Assuming the fluid is istropic and following the similar mathematical derivation as shown in Section 4.2.1 while replacing the deformation by the rate of deformation, the final stress-strain relationship for fluid can be written as:

$$\sigma_{ij} = -P\delta_{ij} + K\dot{\epsilon}_{kk}\delta_{ij} + 2G\dot{\epsilon}'_{ij}$$

OR

$$= -P\delta_{ij} - P_v\delta_{ij} + 2G\left(\dot{\epsilon}_{ij} - \frac{\dot{\epsilon}_{kk}}{3}\delta_{ij}\right) \tag{32}$$

where $P_v = -K\dot{\epsilon}_{kk}$ is called the viscous pressure of the fluid; K and G are the bulk and shear coefficients of viscosity; and the third term in the equation represents deviatoric stress components.

## 5.0 SHOCK WAVES

When a projectile impacts a target, its action is not transmitted instantaneously to all parts of the material body. Shock waves which transmit the deformations and stresses will be generated and radiated out from the impact region with a finite velocity of propagation. There is no disturbance at a point until the stress waves have time to reach that location.

The characteristics of these waves can be obtained by solving the linearized field equation of motion for an infinite elastic medium (Navier's equation).

$$G\nabla^2 u_i + (\lambda + G)\frac{\partial(\nabla u)}{\partial x_i} = \rho\frac{\partial^2 u_i}{\partial t^2} \tag{33}$$

where $\nabla^2 = \frac{\partial^2}{\partial X^2}$ is the Laplace operator; and $\nabla = \frac{\partial}{\partial X_i}$ is the divergence operator.

It can be verified that two solutions satisfying the above equation of motion are:

$$\frac{\partial^2(\nabla u)}{\partial t^2} = V_\ell^2 \nabla^2 (\nabla u) \tag{34}$$

$$\frac{\partial^2 (\omega_k)}{\partial t^2} = V_t^2 \nabla^2 (\omega_k) \tag{35}$$

where $\omega_k$ is the rotation vector and is related to the rotation tensor $\omega_{ij}$ as:

$$\omega_k = \omega_{ij} \frac{1}{2} \left[\frac{\partial u_j}{\partial X_i} - \frac{\partial u_i}{\partial X_j}\right] \tag{36}$$

Both Equation 34 and Equation 35 are exactly the form of wave equations. They are the two kinds of waves representing two different types of body motion and travelling at two different velocities:

$$V_\ell = \sqrt{\frac{\lambda + 2G}{\rho}} = \sqrt{\frac{K + \frac{4}{3}G}{\rho}} \tag{37}$$

$$V_t = \sqrt{\frac{G}{\rho}} \tag{38}$$

where $v_\ell$ is the velocity of longitudinal wave (compression wave, dilatational wave, primary wave, p-wave) in which the particle of the material moves in the same direction as that of wave propagation. The longitudinal wave speed is the speed which sound travels in that material. $V_t$ is the velocity of transverse wave (shear wave, distortional wave, secondary wave, S-wave) in which the particle moves in the dirction perpendicular to that of wave propagation and at a lower speed.

These two types of wave exist without disturbance only in an unbounded elastic continuum. In a finite body, a wave will be reflected when it hits a boundary. If there is another elastic medium beyond the boundary, refracted waves occur in the second medium. An incident longitudinal wave will be reflected and refracted in a combination of longitudinal and transverse waves, and an incident transverse wave will also be reflected in a combination of both types of waves. The detail can be worked out by the proper combination of these waves so that the boundary conditions are satisfied. The reflected longitudinal wave becomes a tensile wave instead of a compressive wave and travels at a speed less than the normal speed of sound. If the compressive

and the shear properties are altered and/or the material becomes inelastic such as due to cracking, yielding and crushing, the followed waves are plastic waves which also travel at a lower speed.

When the stress waves reach a point in the material body, the particle in that location starts to move and the motion shall follow the principles of continuum mechanics. The study of the motion in terms of displacement, velocity, stress, momentum and energy can be computed using the above described field equations while the material properties are continuously revised using constitutive equations to reflect the current physical characteristic of the material under the new stress level.

## 6.0 APPLICATION OF CONTINUUM MECHANICS IN IMPACT PROBLEM

The formulation of field equations and the computational cycle of a typical time step for an impact problem is described herein. It will be demonstrated that the formulation is simply an application of general equations in Section 3. Computation based on Lagrange frame and Euler frame are described separately in the following:

### 6.1 Lagrange Computation

As mentioned earlier, the conservation of mass in Lagrange coordinate system is automatically satisfied. The mass in a zone remains constant. If a zone is deformed and its volume is changed, the new density is then calculated from

$$\rho = \frac{\rho_o \, v_o}{v} \tag{39}$$

where $\rho_o$ and $v_o$ are the initial density and volume of a zone and $\rho$ and v are the new density and volume respectively.

For conservation of momentum, the equation of motion (Equation 7) is applied. Integrating Equation 7 over zone volume results the integral form of equation of motion:

$$a_i = \frac{F_i}{m} \tag{40}$$

Equation 40 is applied at the grid point and is the conventional expression of Newton's law of particle.

With known acceleration, the new velocity and position of grid points can be readily obtained through integration of acceleration and velocity respectively.

Once the velocity is available the strain rate can be computed readily. Given strain rate, the rate of deviatoric stress can be calculated using constitutive equations. If material is elastic (either remain elastic or due to unloading) Hook's law is applied. In such a case Equation 22 is applied.

If material is yielded, the rate of deviatoric stresses have to be obtained through the flow rule discussed in Section 4.2.2.3. No specific equation is given herein because the equations are different depending on the yield model being used.

The new deviatoric stresses are now updated by summing the current value and the incremental deviatoric stresses based on the computed deviatoric stresses rate. Adding the deviatoric stresses to the hydrostatic pressure, the total stresses at current time step can be obtained.

ie. $$\sigma_{ij} = -P\delta_{ij} + \sigma'_{ij} \qquad (41)$$

Note that the pressure P is related to density $\rho$ and specific internal energy e through an equation of state (Equation 16). The $\rho$ is computed from Equation 39 (conservation of mass) and e is from Equation 15 (conservation of energy), where $\dot{e}$ is energy change rate and e is then obtained by adding to the existing specific internal energy an amount of energy change, $\Delta e = \dot{e}(\Delta t)$. It can be found that Equation 15 is also a function of P since the stress components $\sigma_{ij}$ contain P as shown in Equation 41. Equation 15 and 16 represent two independent equations to be solved simultaneously for two unknown, P and e. Once P is found and is substituted into Equation 41, stresses are obtained.

With stress field available, the force can be computed through the integration of stress field over the volume of each zone (see Equation 6). The force of each zone is subsequently divided and applied to the corners (grid points) and/or the interactive boundary points of that zone.

After the force at grid points become available, the computational cycle for next time step starts. A schematic computational cycle of Lagrange processor is shown in Figure A-1.

## 6.2 Euler Computation

In the Euler coordinate system, conservation of mass is enforced through direct application of the equation of continuity (Equation 3) where the first term represents the change of mass in the cell volume and the second term the transport of mass through the cell surface.

For conservation of momentum, Equation 5 is applied.

The computational cycle in Euler is similar to that of Lagrange except that the momentum of the material in a cell is now playing the role as the force in Lagrange and the velocity can now be computed from momentum by simply dividing the momentum by the mass in the cell, ie:

$$V_i = \frac{M_i}{m} \tag{42}$$

Using new material velocity, the mass transport (second term in Equation 3) to a cell can be calcualted as:

$$\Delta m = \rho \vec{V} \cdot \vec{S} \, (\Delta t) \tag{43}$$

the momentum transport (the second term in Equation 5) as:

$$\Delta M_{trans,i} = \rho V_i \, \vec{V} \cdot \vec{S} \, (\Delta t) = V_i \Delta m \tag{44}$$

and the energy transport (the second term on the left hand side of Equation 13 as:

$$\Delta(IE) = \rho e \, \vec{V} \cdot \vec{S} \, (\Delta t) = e \, \Delta m \tag{45}$$

Also, with given velocities, the strain rates can be computed using the known strain rates, the viscous pressure and the deviatoric stresses which represent the second and the third term on the right hand side of Equation 32 can be calculated from their linear relationship to strain rate.

$$P_v = -K \, \vec{\nabla} \cdot \vec{V}$$

$$\sigma'_{ij} = 2G \, (\dot{\varepsilon}_{ij} - \frac{1}{3} \vec{\nabla} \cdot \vec{V}) \tag{46}$$

where the divergence of velocity is related to strain rate as:

$$\vec{\nabla} \cdot \vec{V} = \dot{\varepsilon}_{kk} = \dot{\varepsilon}_{xx} + \dot{\varepsilon}_{yy} + \dot{\varepsilon}_{zz} \tag{47}$$

The total stress as shown in Equation 32 is now evaluated as the sum of a static fluid pressure, a viscous pressure and deviatoric stresses as follows:

$$\sigma_{ij} = -P - P_v + \sigma'_{ij} \tag{48}$$

Again, the pressure P is to be obtained by solving the equation of state and the energy equation simultaneously. Solving Equation 16 and 45 for P and then substituting into Equation 48, stresses are found.

With stress field available, the force can be calculated through integration of stress field over cell surface using Equation 6.

When the applied forces are known, the impulse applied on the cell can be computed by simply multiplying the forces by time increment.

$$\Delta I_{mp,i} = F_i(\Delta t) \tag{49}$$

It can be seen from Equation 5 that the change of momentum in a cell is due to two parts, the momentum transport (Equation 44) and the impulse applied on the cell (Equation 49). Adding the momentum transport and the impulse to the existing value of momentum, the new momentum in a cell is obtained. Then, a new cycle of computation is started from Equation 42. A schematic computational cycle of Euler is shown in Figure A-2.

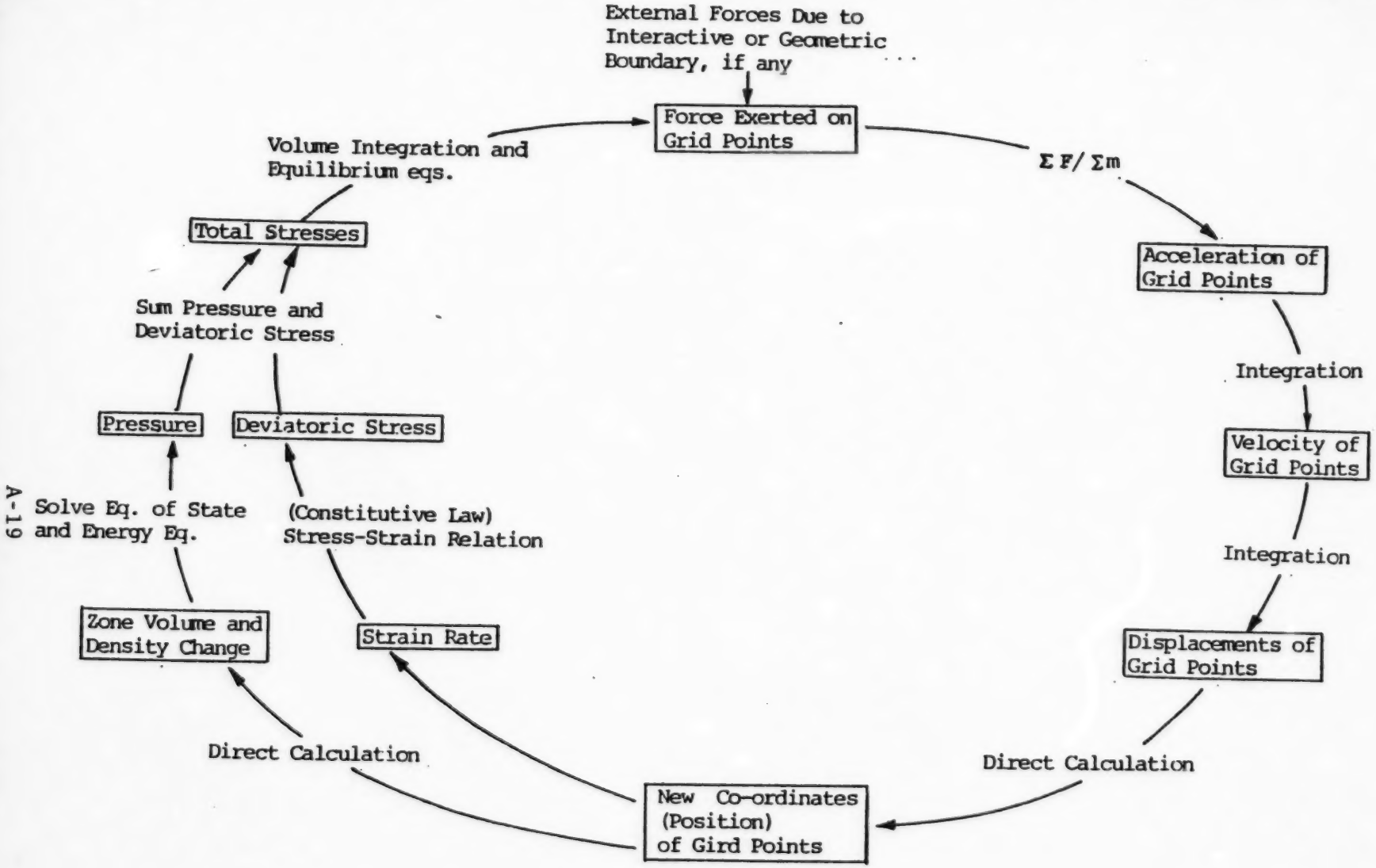


FIG. A1 LAGRANGE COMPUTATION CYCLE

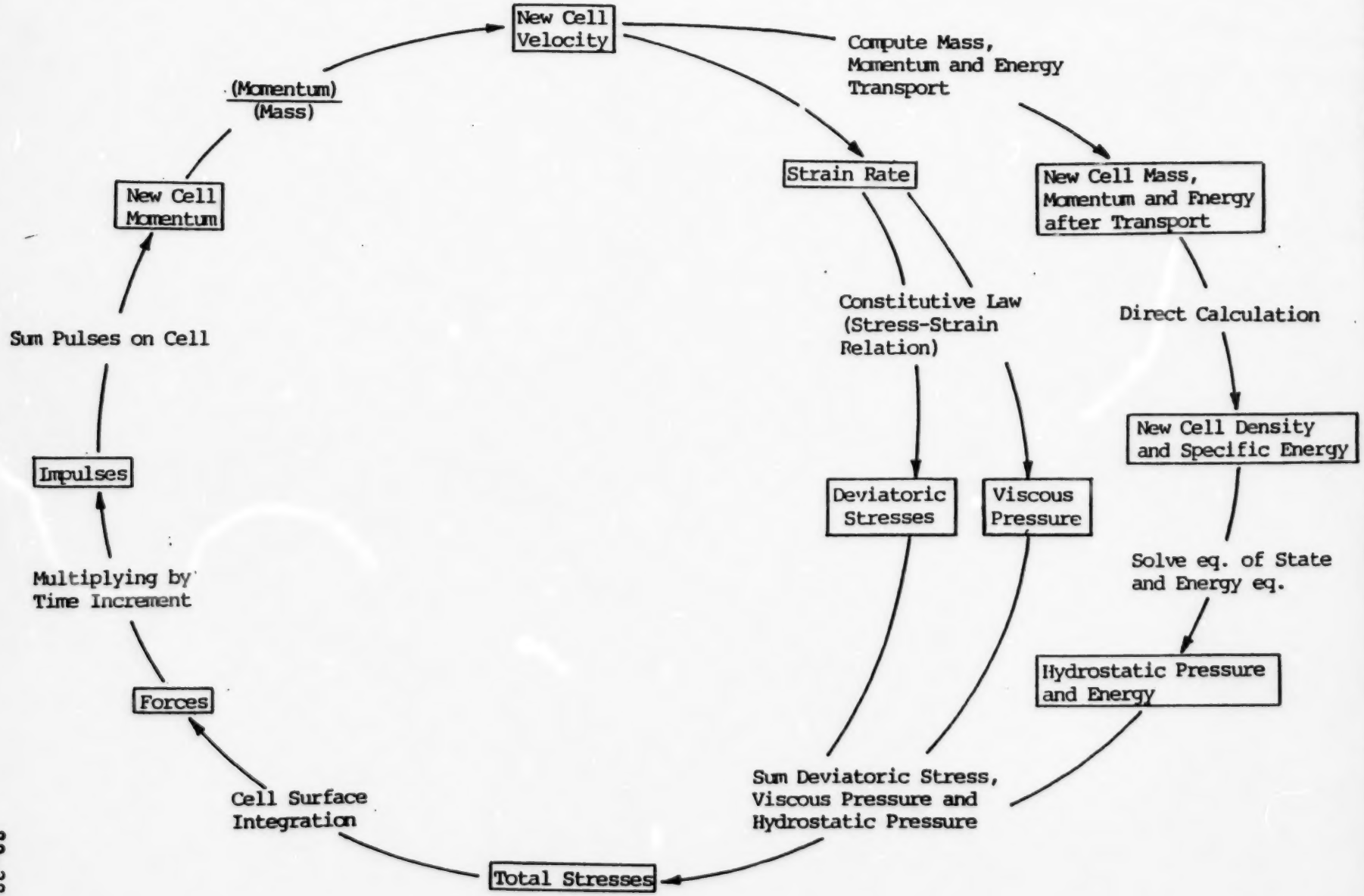


FIG. A2 EULER COMPUTATION CYCLE